Bioactive Materials 36 (2024) 474–489

Contents lists available at ScienceDirect

Bioactive Materials

journal homepage: www.keaipublishing.com/en/journals/bioactive-materials

Tissue-engineered mesenchymal stem cell constructs alleviate tendinopathy by suppressing vascularization

Dijun Li [a,b,c,1], Jingwei Jiu [a,b,1], Haifeng Liu [a,b,1], Xiaojun Yan [d,e], Xiaoke Li [b], Lei Yan [b], Jing Zhang [f], Zijuan Fan [g], Songyan Li [a], Guangyuan Du [a], Jiao Jiao Li [h], Yanan Du [d], Wei Liu [d,e,**], Bin Wang [a,*]

[a] Department of Orthopaedic Surgery, The First Affiliated Hospital, Zhejiang University School of Medicine, Hangzhou, 310006, China
[b] Department of Orthopedics, The Second Hospital of Shanxi Medical University, Taiyuan, 030001, China
[c] Department of Orthopedics, Affiliated Renhe Hospital of China Three Gorges University, Yichang, China
[d] Department of Biomedical Engineering, School of Medicine, Tsinghua-Peking Center for Life Sciences, Tsinghua University, Beijing, 100084, China
[e] Beijing CytoNiche Biotechnology Co. Ltd, Beijing, 10081, China
[f] Department of Emergency Surgery, The Affiliated Hospital of Guizhou Medical University, Guiyang, Guizhou, 550001, China
[g] Department of Health Statistics, School of Public Health, Shanxi Medical University, Taiyuan, 030001, China
[h] School of Biomedical Engineering, Faculty of Engineering and IT, University of Technology Sydney, Sydney, NSW, 2007, Australia

A B S T R A C T

Tendinopathy leads to low-grade tissue inflammation and chronic damage, which progresses due to pathological imbalance in angiogenesis. Reducing early pathological vascularization may be a new approach in helping to regenerate tendon tissue. Conventional stem cell therapy and tissue engineering scaffolds have not been highly effective at treating tendinopathy. In this study, tissue engineered stem cells (TSCs) generated using human umbilical cord mesenchymal stem cells (hUC-MSCs) were combined with microcarrier scaffolds to limit excessive vascularization in tendinopathy. By preventing VEGF receptor activation through their paracrine function, TSCs reduced *in vitro* angiogenesis and the proliferation of vascular endothelial cells. TSCs also decreased the inflammatory expression of tenocytes while promoting their anabolic and tenogenic characteristics. Furthermore, local injection of TSCs into rats with collagenase-induced tendinopathy substantially reduced early inflammation and vascularization. Mechanistically, transcriptome sequencing revealed that TSCs could reduce the progression of pathological angiogenesis in tendon tissue, attributed to Rap1-mediated vascular inhibition. TSCs may serve as a novel and practical approach for suppressing tendon vascularization, and provide a promising therapeutic agent for early-stage clinical tendinopathy.

1. Introduction

Tendinopathy is highly prevalent in athletes and individuals who engage in excessive or repetitive musculoskeletal activities [1,2], with significant impacts on the ability to perform daily activities. Some types of tendinopathy are particularly common, for instance, Achilles tendon symptoms occur in 2–3 per 1000 adult patients, while runners have a 52 % lifetime risk of developing Achilles tendon injuries [3]. Each year, more than 30 million procedures involving tendons are performed worldwide, frequently in athletes, although long-term results are variable [4]. The combined effects of tendinopathy and chronic management place a significant economic burden on the individual and society.

Tendinopathy is an overuse injury characterized by pain and impaired function, presenting microscopically with increased disintegration and alteration of tendon matrix, leading to abnormalities in tendon microstructure, composition, and cell number [5,6]. The primary goal of treatment is to relieve pain symptoms, often through the use of topical or oral anti-inflammatory drugs, while severe tendon injuries may be repaired through surgery [7,8]. These treatment modalities have limited effects on the pathological progression of tendinopathy and may not result in high quality tendon healing, as they do not effectively remodel the injured tissue [9]. Pain is the main symptom of tendinopathy and is thought to be the result of tissue neovascularization [10–13]. Interestingly, despite many investigations on the role of

Peer review under responsibility of KeAi Communications Co., Ltd.
* Corresponding author.
** Corresponding author. Department of Biomedical Engineering, School of Medicine, Tsinghua-Peking Center for Life Sciences, Tsinghua University, Beijing 100084, China.
E-mail addresses: liuwei@cytoniche.com (W. Liu), wangbin_pku@zju.edu.cn (B. Wang).
[1] Dijun Li, Jingwei Jiu and Haifeng Liu are equal first authors.

https://doi.org/10.1016/j.bioactmat.2024.06.029
Received 23 April 2024; Received in revised form 19 June 2024; Accepted 19 June 2024

neovascularization in the pathogenesis of tendinopathy [13,14], a precise link between the two has remained unclear for some time [5,15]. Recent studies have suggested that abnormal vascularization can negatively contribute to tendon injury [5,13], and higher expression levels of angiogenesis-related factors such as vascular endothelial growth factor (VEGF) may be harmful to tendon healing [16]. Research targeting pathological neovascularization as a treatment approach to ameliorate the progression and symptoms of tendinopathy remains limited [5,17].

In recent years, mesenchymal stem cells (MSCs) have been trialed in a small number of studies for treating tendon disorders [18]. It is believed that the anti-inflammatory and analgesic functions of MSCs can target pathophysiological alterations within tissues and produce a permissive microenvironment for tissue regeneration [19,20]. MSC therapy has demonstrated promise in a range of other pathologies, including neurological and musculoskeletal diseases [21], partly due to their ability to upregulate angiogenesis that is critical to the repair of many tissue types. Meanwhile, stem cell therapy alone lacks the ability to regulate tendon tissue differentiation, and practical challenges exist such as maintaining the viability of transplanted cells in the face of mechanical pressure, shearing forces, and limited nutrient supplies [18,22].

Tissue engineering scaffolds have been explored as support structures for cell culture in tendon regeneration, offering tunable mechanical properties and often a biomimetic structure mimicking native tissue features [23,24]. Some biomimetic tendon scaffolds can partly replicate the biomechanical and biochemical elements of the tissue microenvironment to aid regeneration [25]. However, traditional bulk scaffolds require implantation and are more suitable for defect injuries such as tendon rupture, where they provide space filling and tissue support [26]. They are less useful in tendinopathy, which has little demand on mechanical support but greater need for biochemical modulation to promote natural tissue healing and regeneration [27,28]. In comparison, microcarriers can serve as an alternative cell culture and delivery vehicle, providing the ability to control the proliferation and differentiation of loaded stem cells as well as modulating their paracrine activities [29], while still enabling mechanical stimulation of the cultured cells [30]. The microcarriers create a permissive 3D microenvironment that is more conducive to cell-cell communication, matrix deposition, and secretory functions [29,31]. More importantly, in the context of tendon repair, traditional scaffolds with an orderly arrangement tend to promote MSC angiogenic differentiation and tissue revascularization, which is deleterious in tendinopathy [32–34]. In contrast, microcarriers are spherical and dispersed, enabling tight connections to develop among cells, secreted matrix and scaffold, thereby forming microtissue constructs that may effectively limit angiogenesis [35]. Also worth noting is the unique structure of tendon tissue, composed of dense fibrous connective tissue, which creates impediments to simple cell injection. Unlike in intra-articular and intraperitoneal injections, direct cell delivery into tendons is prone to immediate extrusion from the tissue and hence significantly reduced therapeutic impact [22]. *In vivo* stem cell delivery using microcarriers not only benefits from a 3D culture platform that can preserve stem cell characteristics, but also better ability to integrate with host tissue and protect cells from tissue extrusion [36].

Human umbilical cord MSCs (hUC-MSCs), with minimal immunogenicity, high capacity for proliferation and differentiation, and significant ability to give rise to tendon-like cells, may have great potential for clinical application compared to other tissue sources in cell-based tendon repair [37–39]. In our previous research, hUC-MSCs have shown minimal immunogenicity or other complications when applied to rat models of osteoarthritis [36] and spinal cord injury [29]. In response to mechanical stimulation, hUC-MSCs have also shown the ability to accelerate early tendon tissue reconstruction and healing, particularly by increasing extracellular matrix (ECM) formation and restoring native tendon tissue structure [40,41]. In this study, we for the first time combined the advantages of hUC-MSCs and microcarrier scaffolds to construct tissue-engineered stem cells (TSCs), utilizing our previous experience with injectable gelatin microcarriers as a robust stem cell culture platform [36]. The gelatin microcarriers were created by cross-linking gelatin using glutaraldehyde, resulting in macroporous structures with fully interconnected pores of 30–80 μm and high porosity above 95 %, as well as tunable mechanical properties in the 20–200 kPa range suitable for cell culture and ECM formation [42,43]. Gelatin microcarriers loaded with cells have been shown to form microtissues, maintaining structural integrity while improving the therapeutic function of cells. For instance, MSCs grown within gelatin microcarriers have demonstrated modifications in paracrine activity and hence altered repair outcomes in different disease models [36,44], suggesting that the functions of these microcarrier scaffolds extend beyond a simple cell growth or delivery platform to facilitate the formation of tissue engineered MSC constructs.

In this study, suppressing the pro-angiogenic functions of endothelial cells and leading to better phenotype maintenance of tenocytes *in vitro*, as well as promoting tendon restoration *in vivo* in a rat Achilles tendon injury model through histological, biomechanical, and functional analyses. This study offers a comprehensive understanding of how TSCs can regulate healing in tendinopathy, and presents an improved stem cell-based strategy for tendon tissue engineering.

2. Results

2.1. Preparation and characterization of TSCs

hUC-MSCs were grown in gelatin microcarriers to construct the TSCs. The shape and size of microcarriers were imaged using scanning electron microscopy (SEM), showing 3D microporous structures with pore sizes of 10–30 μm and diameter of approximately 200 μm (Fig. S1, Supporting Information). The 3D porous structure of spherical microcarriers provides high surface area for cell culture, while facilitating nutrient diffusion and cell-cell interactions. Calcein AM/PI live/dead staining showed that MSCs seeded on microcarriers survived and continued to proliferate over 5 days (Fig. 1A).

The senescence, proliferation, and tenogenic potential of MSCs were compared for cells grown in 3D microenvironment within TSCs to those grown using traditional 2D adherent culture. Cells within TSCs showed improved viability than those grown in 2D from day 3 of culture (Fig. S2, Supporting Information). Cells in TSCs showed comparatively lower oxidative stress than MSCs in 2D (Fig. 1B, Fig. S2, Supporting Information). TSCs also showed reduced senescence as seen through less β-galactosidase staining (Fig. 1C and D), and significantly down-regulated expression of the senescence-related genes P16 on day 1, and *P21* over 5 days (Fig. 1G). EDU fluorescence staining indicated significantly higher cell proliferation in TSCs compared to MSCs in 2D from day 3 onwards (Fig. 1E and F). Interestingly, cell proliferation was higher in the MSCs group compared to TSCs on day 1 (Fig. 1E). This was likely because on the first day of culture, MSCs were freshly transplanted to gelatin microcarriers to form TSCs, and needed time to acclimatize to the new 3D culture environment from traditional 2D monolayer culture on plastic. At day 3 and beyond, rapid proliferation occurred in the TSCs after the cells have adapted to the new 3D environment within microcarriers that is more conducive to cell activity. Tenogenic potential was elevated in MSCs grown in TSCs, as shown through the significantly higher expression of tendon-related genes mohawk (*MKX*) and scleraxis (*SCX*) (Fig. 1H). These findings suggest that growing MSCs in 3D within microcarriers can enhance cell survival and proliferation, reduce senescence, and improve tenogenic differentiation potential.

2.2. TSCs suppress the pro-angiogenic functions of endothelial cells

MSCs are known to alter their biological functions such as paracrine signaling in response to the culture microenvironment and substrate [45], although specific investigations particularly on the secretome level

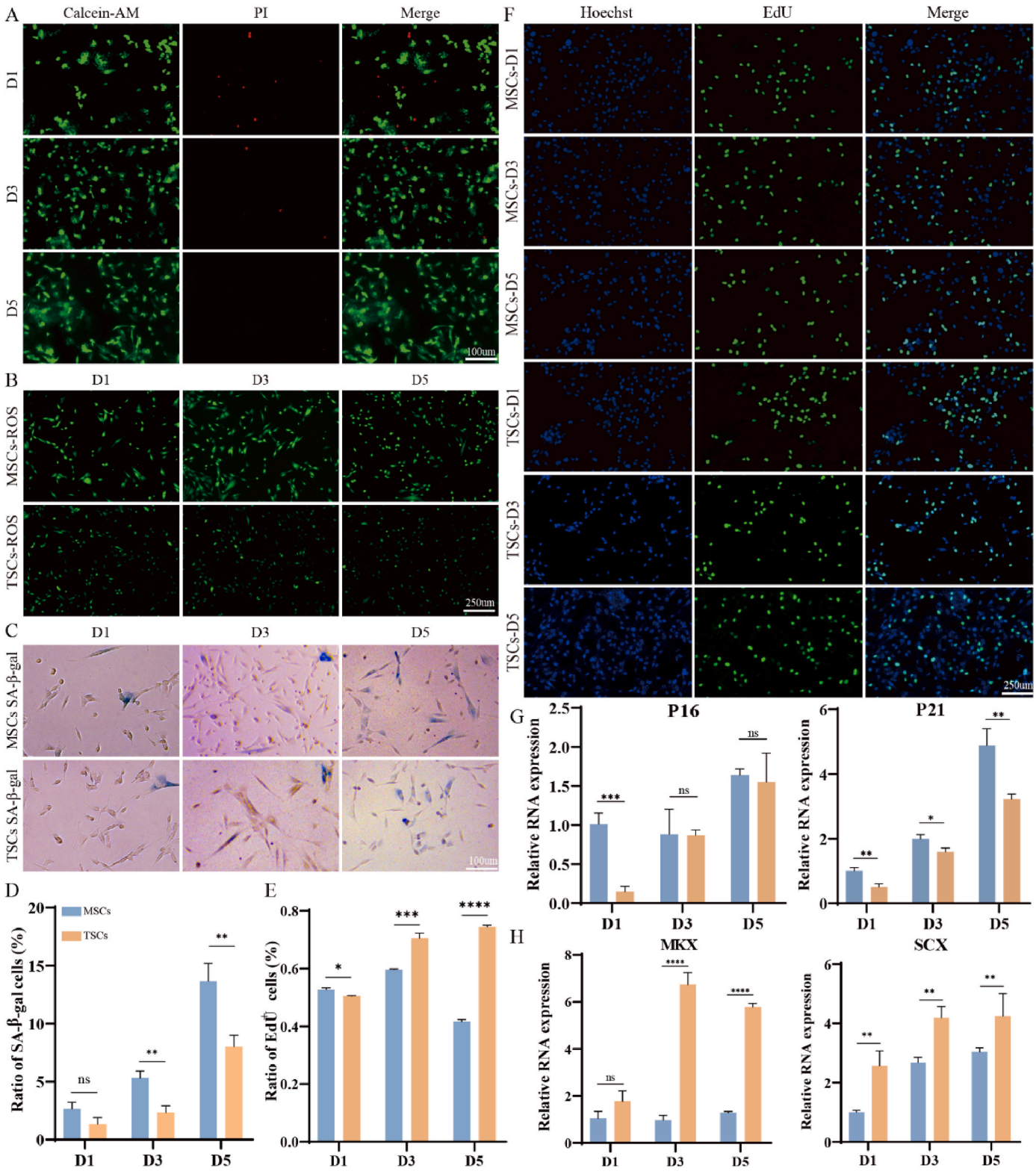

Fig. 1. Characterization of TSCs. (A) Live/dead staining fluorescence images of 3D TSCs on day 1, 3, and 5 of culture (scale bar = 100 μm). (B) Reactive oxygen species (ROS; scale bar = 250 μm) and (C) senescence staining images (scale bar = 100 μm). (D) Quantification of β-galactosidase staining and (E) cell proliferation by EDU at 1, 3, and 5 days. (F) Fluorescence images of EDU cell proliferation assay (scale bar = 250 μm). (G) Relative expression levels of genes for senescence (*P16*, *P21*) and (H) tenogenic differentiation (*MKX*, *SCX*). Results are presented as mean ± SD. Unpaired two-tailed student's t-test or Mann-Whitney *U* test was used for statistical analysis. *p < 0.05, **p < 0.01, ***p < 0.001, and ****p < 0.0001; n = 3.

remain limited. In this study, secretome analysis was conducted using culture supernatants from the 3D TSCs and 2D MSCs groups. GO and KEGG analyses (Fig. 2A and B) suggested that MSCs within TSCs had significant alteration in molecular pathways related to vascularization and angiogenesis. To investigate the specific paracrine effects of TSCs on angiogenesis, the human endothelial cell line Ea. hy926 was used to perform related assays, after being exposed to conditioned medium (CM) obtained from culturing TSCs or 2D MSCs (Fig. 2C). Endothelial cells grown in CM from TSCs showed reduced protein expression of VEGF receptor (VEGFR1), a marker of angiogenesis, and proliferating cell nuclear antigen (PCNA), a marker of cell proliferation (Fig. 2D; Fig. S3, Supporting Information). Functional angiogenic assays showed that endothelial cells treated with CM from TSCs formed a lower number of capillary tube-like structures, with decreased total tube length and branch points, compared to those treated with CM from 2D MSCs (Fig. 2E–G). Moreover, the results of both the transwell assay (Fig. 2F–I) and scratch wound assay (Fig. 2H–J) revealed significant inhibition of endothelial cell migration by CM from TSCs. Hence, the secretory products of MSCs grown in TSCs may inhibit the process of vascularization by suppressing the angiogenic function of endothelial cells.

2.3. TSCs lead to better phenotype maintenance of tenocytes in an in vitro model of tendinopathy

MSCs delivered through biomaterial platforms [46,47], including using gelatin microcarriers [29] have shown improved paracrine functions that contribute to modulating cellular behaviour and promoting tissue repair. However, there is limited evidence on the paracrine effects of MSCs delivered through microcarriers in tendinopathy. A transwell co-culture model of tendinopathy was set up by growing primary tenocytes (TC) isolated from rat Achilles tendon (Figs. S4A–C, Supporting Information) [48,49] together with TSCs or MSCs in 2D, separated by the transwell membrane whereby different cell types cannot contact each other but share the same culture medium (Fig. 3A). The co-cultures were stimulated with IL-1β for 48 h to simulate inflammatory conditions in tendinopathy [50]. Compared to tenocytes grown under normal culture conditions (NC), tenocytes stimulated with IL-1β (TEN) showed marked reduction in the expression of tenogenic marker tenascin-C (*TNC*), although the expression levels of other tenogenic markers were similar between NC and TEN (Fig. 3B). TNC, fibromodulin (*FMOD*) and tenomodulin (*TNMD*) all perform critical roles in collagen fibril production and assembly, as well as tendon maturation, and are commonly used as later stage markers of tendon formation or repair. Tenocytes stimulated with IL-1β and co-cultured with TSCs (TC-TSCs) or MSCs in 2D (TC-MSCs) showed significant elevation in the expression levels of all three tenogenic markers, pointing to the paracrine effects of MSCs in promoting phenotype maintenance in tenocytes under inflammatory conditions simulating tendinopathy irrespective of whether the MSCs were grown in a 2D or 3D environment.

Collagen type I (COLI) is the primary collagen comprising tendon tissue, and its expression was significantly reduced in the TEN group but largely restored in the TC-MSCs and TC-TSCs groups (Fig. 3C). Meanwhile, as a marker of tendinopathy, collagen type III (COLIII) was greatly elevated in the TEN group compared to NC, but levels were reduced in the TC-MSCs group and restored to levels comparable to NC in the TC-TSCs group (Fig. 3D). The expression levels of matrix metalloproteinases (MMPs) as catabolic markers (MMP3 and MMP13) were also examined as indicators of tendon degradation under inflammatory conditions (Fig. 3E and F). Both markers were dramatically elevated in the TEN group compared to NC, and interestingly, the TC-MSCs group was ineffective at reducing the expression of these catabolic markers. In contrast, the TC-TSCs group achieved dramatic reduction in the expression of both MMP3 and MMP13 compared to TEN, to levels matching the NC group. These observations are confirmed by quantitative results from the staining images (Fig. 3G). The findings suggest that MSCs grown in 2D or 3D can exert substantial paracrine effects to modulate inflammation in tendinopathy, leading to better preservation of tissue structure. The MSCs grown in 3D within microcarriers had better ability to inhibit tendon tissue degradation by suppressing the production of catabolic proteins, while the MSCs grown in conventional 2D culture showed more limited effects.

2.4. TSCs improved sensory and motor function in rats with induced tendinopathy

The rat tendinopathy model was established by intermittent injections of type I collagenase [51] in the Achilles tendon for 2 weeks (Figs. S5A–B, Supporting Information) to induce tendon damage. MSCs or TSCs were injected into the tendon at 2 weeks, and the animals were sacrificed at 4 weeks following the treatment (Fig. 4A and B). Prior to sacrifice, the rats were subjected to pain threshold [52] and lower limb contact pressure [53] measurements (Fig. S5C, Supporting Information). Rats in the untreated tendinopathy group had a significantly reduced pain threshold compared to the unoperated control, while groups treated with MSCs or TSCs restored the pain threshold to levels approaching the control (Fig. 4C). Similar trends were seen for the lower limb contact pressure (Fig. 4D). For both measurements, the TSCs group showed an improved level of pain tolerance compared to the MSCs group.

Assessment of motor function revealed that both MSCs and TSCs treatment groups resulted in better hind limb movement compared to the tendinopathy group, with measurement levels approaching those of the control. Specifically, both treatment groups showed significant reduction in gait cycle, more coordinated motion, and increase in average walking speed (Fig. 4E and F). Moreover, the treatment groups dramatically increased their standing duration and floor contact area, as well as running duration (Fig. 4G, Fig. S5D, Supporting Information). The majority of measured motor parameters were improved to a greater extent in the TSCs group compared to MSCs.

2.5. TSCs can improve tendon repair and minimize disease characteristics of tendinopathy

Gross observation of the collected tissue samples after sacrificing showed significant tendon atrophy and thinning in the tendinopathy group (Fig. 5A). Upon closer observation, the degree of adhesion as an indication of disease was greatly elevated in the tendinopathy group, which was also reflected by the adhesion score [54] (Fig. 5A–D). The injection of TSCs or MSCs effectively reversed the gross pathological changes seen in the tendinopathy group, restoring the macroscopic appearance of the tendon to represent the control group.

Masson staining revealed substantial tissue thickening in the tendinopathy group, accompanied by disorganization of ECM, inflammatory cell infiltration, and collagen fiber edema (blue-stained areas) (Fig. 5B). These microscopic pathological features of tendinopathy were largely reversed in the TSCs and MSCs groups, with the TSCs group exhibiting greater improvements, which was also reflected through its significant reduction in collagen volume fraction compared to both the tendinopathy and MSCs groups (Fig. 5E). Hematoxylin-eosin (HE) staining verified the restoration of histological tendon structure in the TSCs and MSCs groups approaching the control, although with a higher cell mass than the native tendon (Fig. 5C). Both treatment groups showed transverse aligned fibrous tissue, in stark contrast to the randomly organized fibers in the tendinopathy group, as well as a lower degree of cellular infiltration and higher density of spindle-shaped cells. Meanwhile, the TSCs group showed the lowest degree of vascularization (with red arrows indicating tiny vessels). Histological scores [30] for fiber structure, fiber arrangement, nuclear round degree, inflammatory cells, number of blood vessels, and number of cells were significantly improved in both treatment groups, with the TSCs group showing overall better scores more closely resembling the control (Fig. 5F). These findings collectively suggest that TSCs might enhance tendon

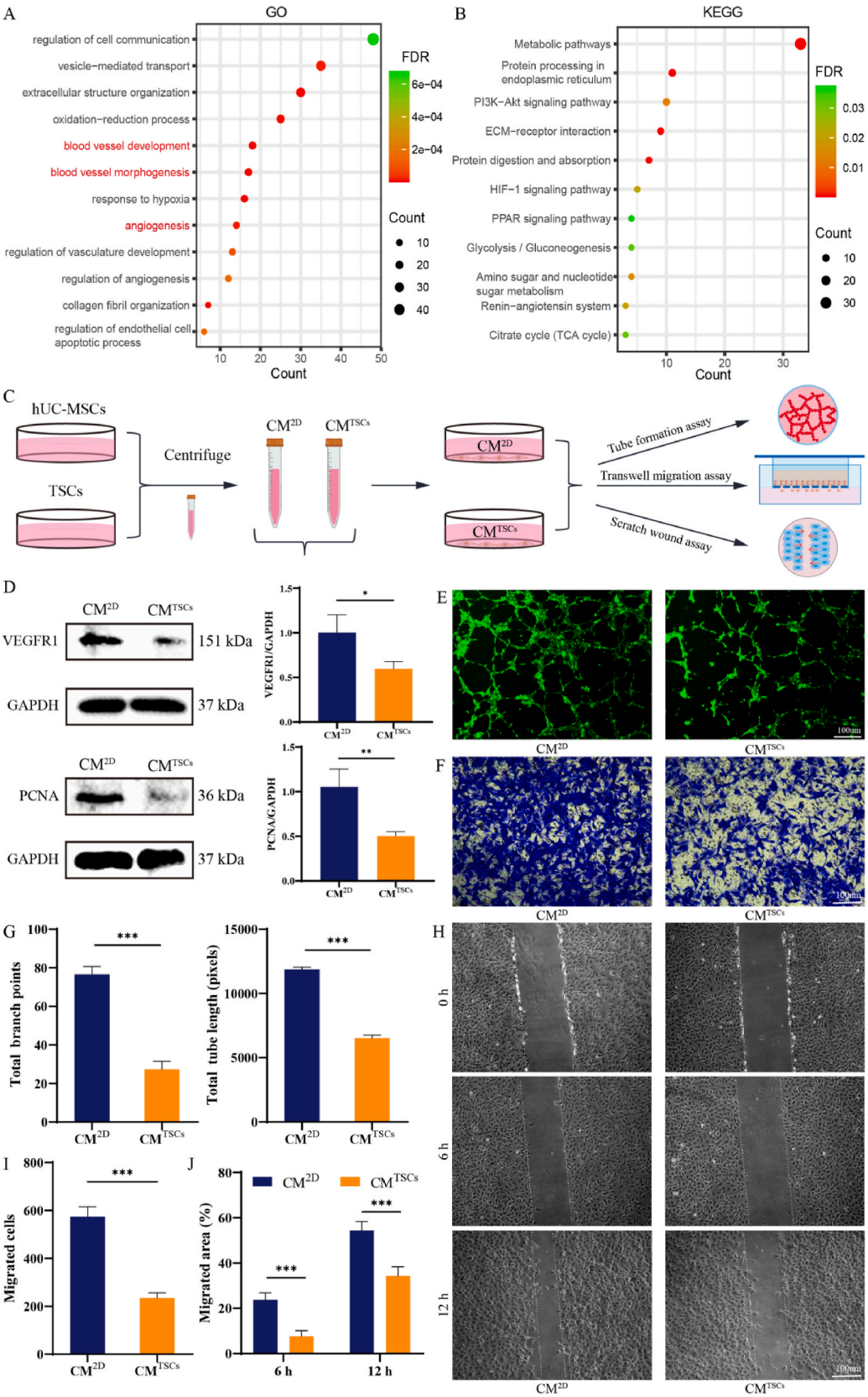

Fig. 2. Evaluation of the angiogenic function of human endothelial cells (Ea.hy926) in the presence of CM^{TSCs} or CM^{MSCs}. (A) Proteomic analysis of GO enrichment analysis and (B) KEGG analysis of culture supernatants from TSCs and MSCs groups. (C) Experiment design for functional angiogenic assays performed using human endothelial cells. (D) Western blot analysis of VEGF receptor (VEGFR1) and proliferation marker (PCNA) expression in endothelial cells treated with TSC and MSC supernatants. (E) Representative images and (G) quantification of tube formation by endothelial cells stimulated with CM from each group. Scale bar = 100 μm. (F, I) Transwell assay and (H, J) scratch wound assay to evaluate endothelial cell migration for each group. Scale bar = 100 μm. Results are presented as mean ± SD. Unpaired two-tailed student's t-test or Mann-Whitney *U* test was used for statistical analysis. *$p < 0.05$, **$p < 0.01$, ***$p < 0.001$, and ****$p < 0.0001$; $n = 3$.

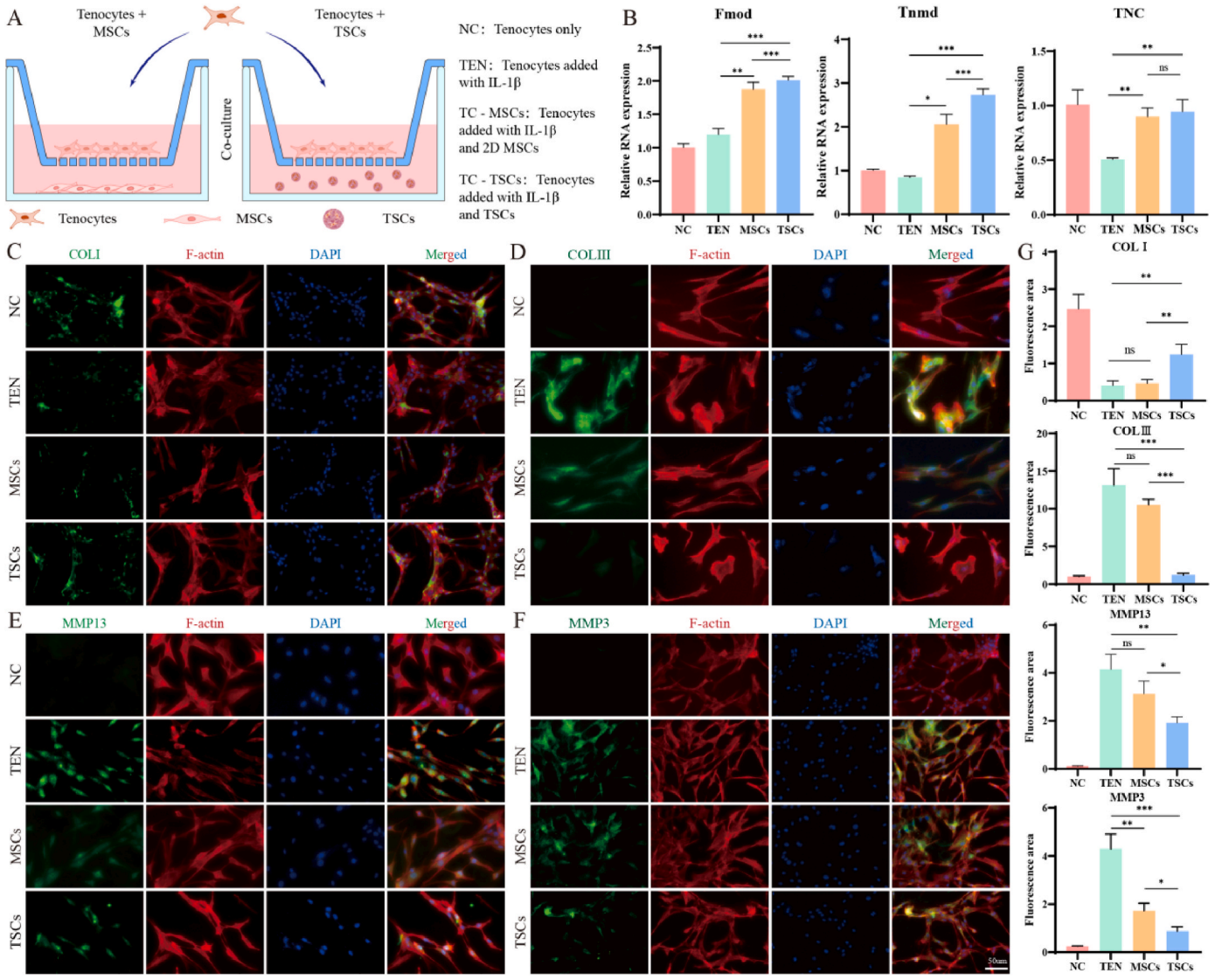

Fig. 3. Evaluation of the paracrine effects of TSCs and 2D MSCs on tenocytes in an *in vitro* model of tendinopathy. (A) Schematic illustrating the co-culture system of tenocytes with TSCs (TC-TSCs) or 2D MSCs (TC-MSCs), stimulated with IL-1β to simulate inflammation in tendinopathy. (B) Relative expression of tenogenic markers (*FMOD*, *TNMD*, *TNC*) after co-culture. Immunofluorescence staining images of (C) COLI, (D) COLIII, (E) MMP3, and (F) MMP13 (scale bar = 50 μm), and (G) quantitative results, after 48 h of co-culture. Results are presented as mean ± SD. One-way ANOVA with Tukey's multiple comparisons or Kruskal-Wallis H-test with Dunn's multiple comparisons was used for statistical analysis. *p < 0.05, **p < 0.01, ***p < 0.001, and ****p < 0.0001; n = 3.

regeneration by lowering tissue adhesion and edema, while also modulating the inflammatory microenvironment following tendon damage. Although both treatment groups exhibited notable tendon repair, the TSCs group showed better restoration of native tissue structure compared to the MSCs group.

2.6. TSCs inhibited tendon vascularization and matrix degradation, and increased tenogenic ability

Collected tendon tissue was stained to detect markers of neovascularization as a pathogenic hallmark of tendinopathy, including VEGF as well as CD34 as a specific target of vascular endothelial cells (Fig. 6A and B). Both markers were strongly expressed in the tendinopathy group, followed by reduced but still high expression in the MSCs group, but were significantly downregulated in the TSCs group (Fig. 6G), suggesting that TSCs treatment was effective at reducing diseased vessel formation. Simultaneously, apoptosis and proliferation of local tissues were significantly reduced in the treatment groups compared to the tendinopathy group (Fig. S6, Supporting Information).

COLI is the main collagen in healthy tendon fibers, while COLIII tends to accumulate at the onset of tendinopathy. Staining of both collagens indicated profound reduction of COLI in the tendinopathy group accompanied by increase in COLIII content, which were restored to levels closer to normal in the treatment groups, with the TSCs displaying more enhanced effects at tendon regeneration and restoring native fiber composition (Fig. 6C and D). Meanwhile, staining for MMP3 and MMP13 were notably reduced in the treatment groups compared to the tendinopathy group (Fig. 6E and F), with the TSCs group showing lower levels of expression than MSCs, suggesting it was more effective at inhibiting tendon matrix catabolism and enabling repair. The trends in expression levels of COLI, COLIII, MMP3 and MMP13 among groups from the *in vivo* model matched those found using the *in vitro* co-culture model of tendinopathy.

2.7. mRNA sequencing shows TSCs enhanced tendon remodeling by suppressing vascularization

All *in vivo* outcomes suggested that the TSCs treatment group had the

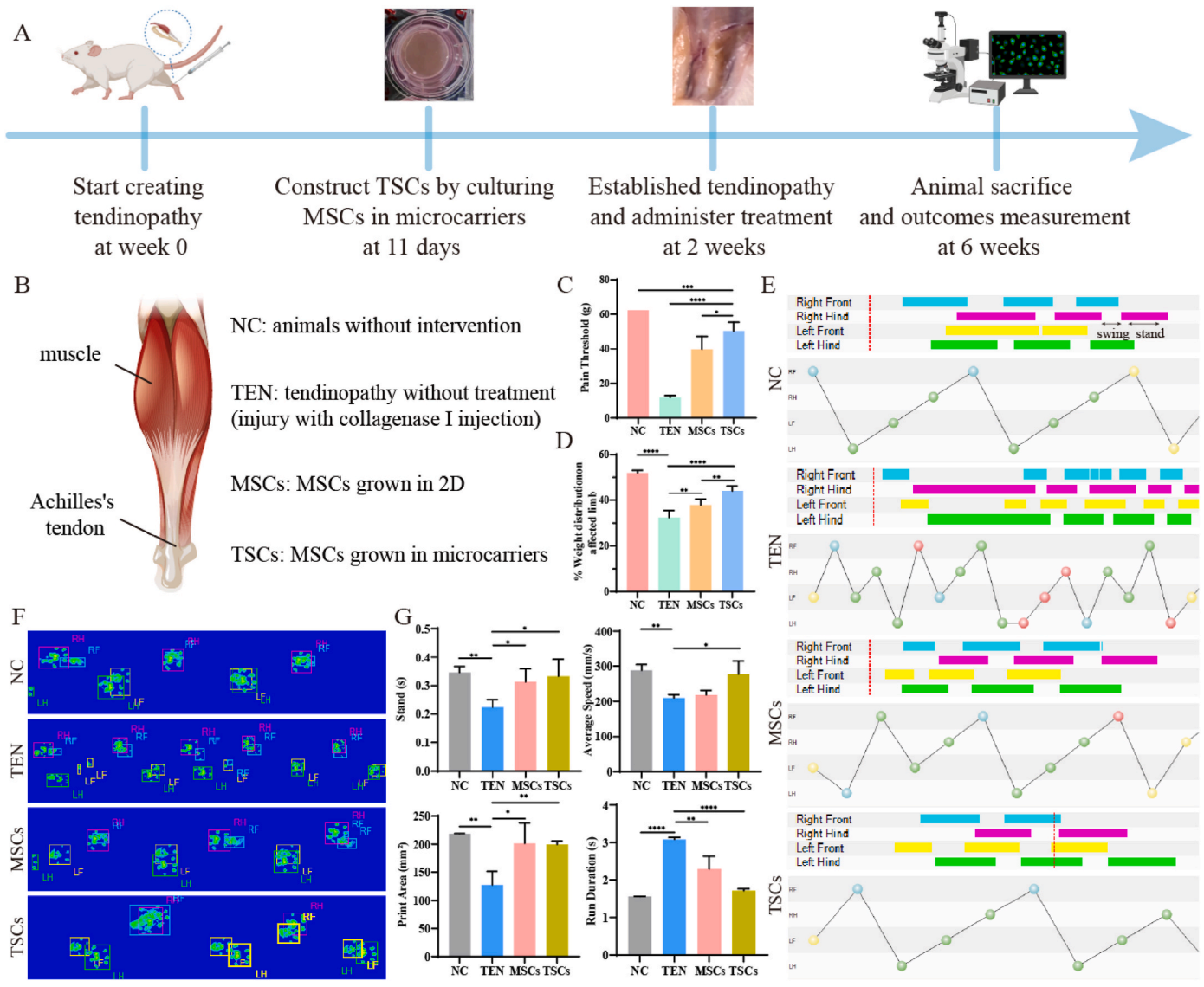

Fig. 4. Behavioral tests were performed after 4 weeks of treatment with TSCs or MSCs in a rat model of tendinopathy induced by type I collagenase injection. (A) Timeline for the *in vivo* experiment. (B) Schematic illustration of the experiment groups. (C) Change in lower limb pain threshold and (D) contact pressure at 4 weeks after treatment. (E–G) Gait analysis and quantification results of hind limb motor function. Results are presented as mean ± SD. One-way ANOVA with Tukey's multiple comparisons or Kruskal-Wallis H-test with Dunn's multiple comparisons was used for statistical analysis. *p < 0.05, **p < 0.01, ***p < 0.001, and ****p < 0.0001; n = 3.

best effects at encouraging tissue repair in tendinopathy. mRNA-seq analysis was used to gain mechanistic insights into tendon healing enabled by TSCs in comparison to the tendinopathy group. Principal component analysis (PCA) indicated substantially different patterns of gene expression in the TSCs group compared to the tendinopathy group, including 388 downregulated and 271 upregulated differentially expressed genes (DEGs) (Fig. 7A and B). Some of the major GO functions of DEGs involved in tendon regeneration were extracellular matrix organization, myoblasts differentiation, and vascular associated smooth muscle cells proliferation (Fig. 7C). In addition, a marked drop was noted in the enrichment of genes associated with blood vessels (THBS1, NOTCH3, and IGFBP5), which control the proliferation and migration of vascular cells (Figs. S6A–B, Supporting Information). KEGG enrichment analysis showed significant downregulation of signaling pathways associated with MAPK, Rap1, and vascular smooth muscle contraction, as well as significant upregulation of AMPK, PPAR, and adipokine signaling pathways (Fig. 7D). All of these molecular pathways are associated with immunomodulation and vascularization, suggesting that the MSCs grown within TSCs regulated tendon repair by means of these processes. Single-gene GSEA enrichment analysis was further used to specifically investigate the vascularization gene VEGF-A, showing that it was significantly enriched in the control of tissue remodeling and oxidoreductase complexes (Fig. 7E). Furthermore, the tenogenic-related genes TNMD and DCN and inflammation-related genes IL-1β and IL-6 were enriched in the control of immunity and vascularization (Figs. S7C–D, Supporting Information). Immunofluorescence staining further confirmed that Rap1 expression in the TSCs group was much lower than in the tendinopathy group, and expression levels were elevated in locations with high VEGF expression (Fig. 7F). Further details of the mRNA-seq analysis are presented in Fig. S8, Supporting Information.

3. Discussion

This study investigated for the first time the utility of TSCs, comprising integrated constructs of MSCs in a microcarrier matrix, in

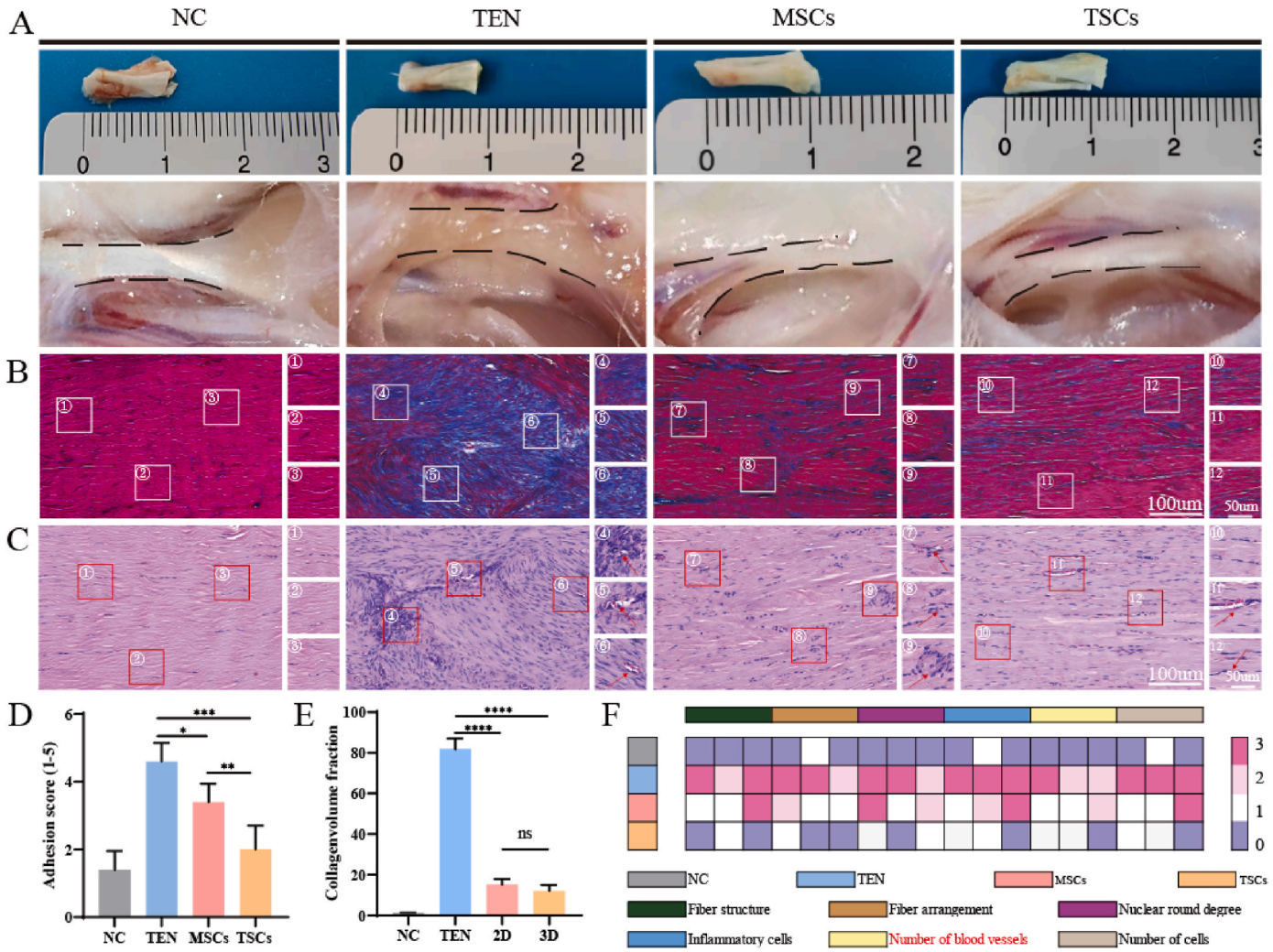

Fig. 5. TSCs improved tendon repair and regeneration in a rat model of tendinopathy. (A) Macroscopic observation of explanted tendon at 4 weeks after treatment. Representative images of (B) Masson staining and (C) HE staining (red arrows indicate tiny vessels). Scale bar = 100 μm. Scale bar = 50 μm. Relative quantification of (D) adhesion score, (E) collagen volume fraction, and (F) histological scores. Results are presented as mean ± SD. One-way ANOVA with Tukey's multiple comparisons or Kruskal-Wallis H-test with Dunn's multiple comparisons was used for statistical analysis. *p < 0.05, **p < 0.01, ***p < 0.001, and ****p < 0.0001; n = 3.

repairing damaged tendon tissue using *in vitro* and *in vivo* models of tendinopathy. Compared with MSCs grown by traditional 2D culture, TSCs exhibited the unique ability to inhibit cell and tissue inflammation, effectively modulating the local microenvironment and creating more permissive conditions to enable tendon repair while preventing further pathological progression. *In vitro*, the culture supernatant of TSCs containing their secretory products was able to suppress vascular endothelial cell angiogenesis, a critical factor driving the pathogenesis of tendinopathy, while promoting matrix anabolism. *In vivo*, TSCs administered in a rat model of tendinopathy showed ability to enable restoration of tissue structure and ongoing tendon repair, including the suppression of inflammatory response and inhibition of vascularization. Transcriptome bioinformatics analysis confirmed the associated molecular pathways as the mechanisms driving tissue repair and regeneration.

Microcarrier scaffolds may provide significant benefits in tissue regeneration by supporting cell growth and regulating cell activity. However, our previous studies using a similar microcarrier system that constructed microtissues involving MSCs for different disease applications showed minimal tissue healing effects conferred by the empty microcarriers without cells [29,44]. In those studies, the injected empty microcarriers would be quickly dispersed and unable to integrate into the host tissue at the damage site. In this study, we constructed TSCs by combining the advantages of umbilical cord-derived MSCs and microcarriers. The use of microcarriers as a culture platform for MSCs to form TSCs presents several advantages for tendon repair. Firstly, the porous and microscopic structure of microcarriers allow loaded MSCs to be grown in a 3D environment that more closely resembles their native niche, permitting ECM formation and intercellular communication that are essential for preserving MSC viability and function [55]. Following *in vivo* implantation, the TSCs could function as autonomous units to integrate with injured tendon, effectively preventing cell loss due to extrusion from the thick and dense tendon fiber bundles. The better preservation of MSC function within TSCs reduces local oxidative stress and improves paracrine effects, all of which contribute to tendon tissue regeneration and remodeling. Secondly, stem cells naturally exist in a 3D mechanical microenvironment whereby the intrinsic mechanical characteristics of ECM are an essential influencing factor driving stem cell behavior and fate [56]. Compared to direct stem cell injection, TSCs provide a 3D environment that adds mechanical conditioning to MSCs while also protecting them from the significant shear stresses encountered during needle injection. Other studies have shown that microenvironmental mechanics can help stimulate tenogenic differentiation in stem cells at moderate stiffness [57,58]. Moreover, specially designed 3D scaffolds with tunable mechanical properties such as elastic modulus can directly influence stem cell behavior and enhance the expression of

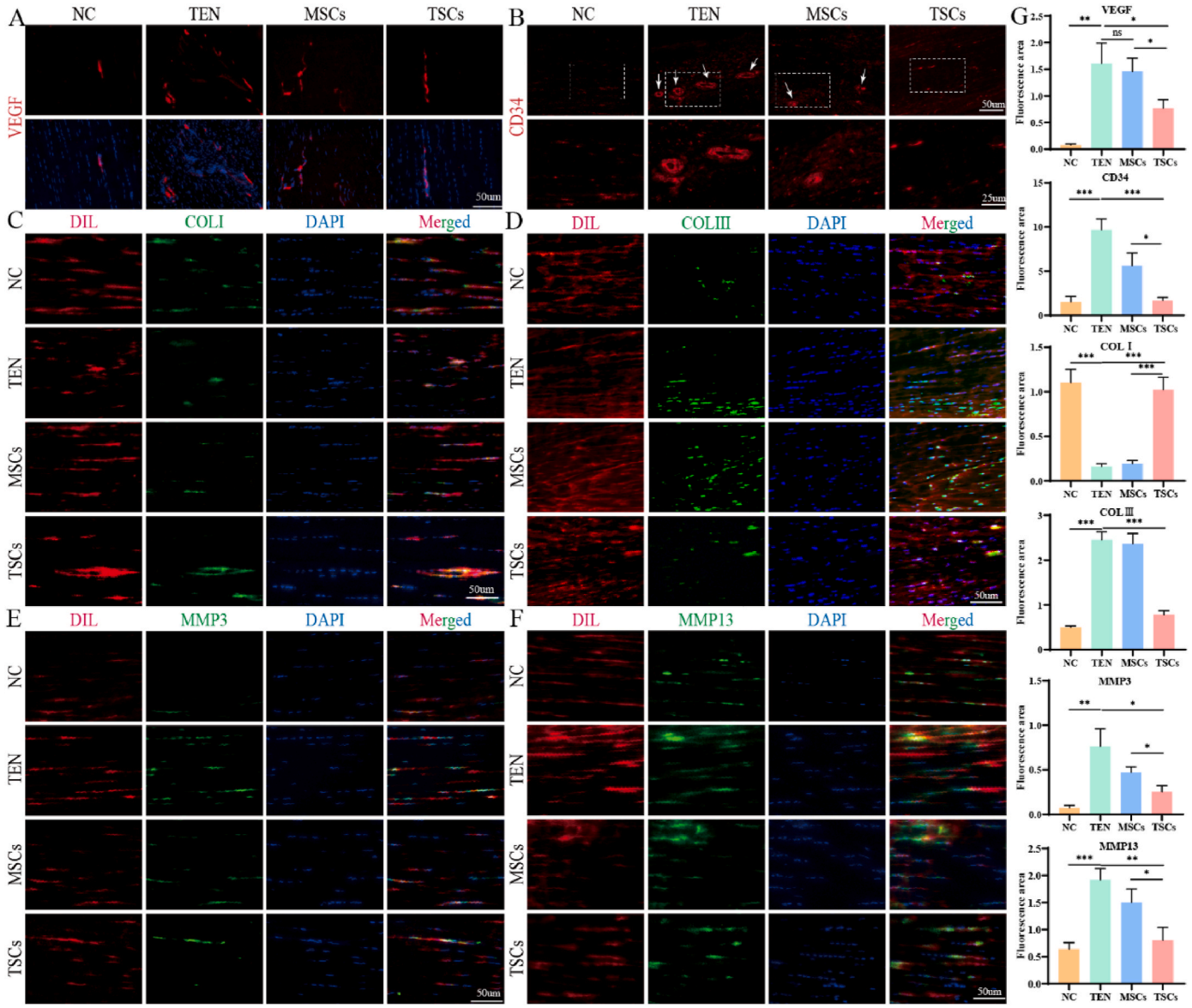

Fig. 6. TSCs suppress tissue vascularization while promoting matrix formation in a rat model of tendinopathy. Immunofluorescence staining of (A, B) vascularization indicators (CD34 and VEGF), upper scale bar = 50 μm, lower scale bar = 25 μm. (C–F) Anabolic (COLI) and disease/catabolic (COLIII, MMP3, MMP13) indicators, scale bar = 50 μm. (G) Quantification of relative staining intensity. Results are presented as mean ± SD. One-way ANOVA with Tukey's multiple comparisons or Kruskal-Wallis H-test with Dunn's multiple comparisons was used for statistical analysis. *p < 0.05, **p < 0.01, ***p < 0.001, and ****p < 0.0001; n = 3.

tenogenic markers [59,60]. Our earlier investigation suggested that the microcarrier scaffolds utilized in this study had moderate stiffness (Young's modulus of 16 kPa) suitable for tuning stem cell behavior [59]. Aligning with the effects of substrate stiffness on MSC behavior observed in other studies, our current investigation showed that the microcarriers could stimulate tenogenic differentiation of MSCs.

The 3D structure and mechanical conditioning provided by microcarriers could act synergistically to enhance MSC function and paracrine activity [36]. Specifically, the mechanical stimulation introduced by microcarriers could promote the activation of mechanosensing pathways and associated factors such as YAP, which could contribute to improving MSC paracrine activity [61]. Secretome analysis in previous studies have indicated that MSCs grown in a 3D scaffold have increased secretory function, including for beneficial molecules such as FGF7 that plays a crucial role in tendon regeneration following injury [30]. Our earlier research also demonstrated significant changes in the paracrine activity of MSCs grown in 3D microcarrriers, including modulation in the levels of cytokines with proliferative, immunomodulatory, and angiogenic functions [44]. Similar mechanisms may be at play in the TSCs of our study, whereby transcriptome sequencing confirmed the enhanced paracrine effects of cells within TSCs. These paracrine effects are shown to be at least partly mediated by intercellular communication pathways including extracellular vesicles. The enhanced MSC paracrine signaling has translated to improved tendon repair, involving processes such as reduced inflammation, as well as increased myoblast differentiation and ECM remodeling, which have been confirmed by sequencing analyses. Notably, suppressing the early inflammatory response in tendinopathy is a key to recovery [62], pointing to the important role of TSCs in kick-starting tissue repair through reducing inflammatory expression while promoting matrix reorganization.

Tendinopathy is a broad term describing a range of changes that occur in damaged and diseased tendons, leading to pain and decreased function [5]. In this study, collagenase injection was chosen to model *in vivo* tendon disease because it not only induces local inflammation of tendon tissue, but also mimics the loss of collagen that occurs during tendinopathy [63], as well as pathological vascularization. Collagenase

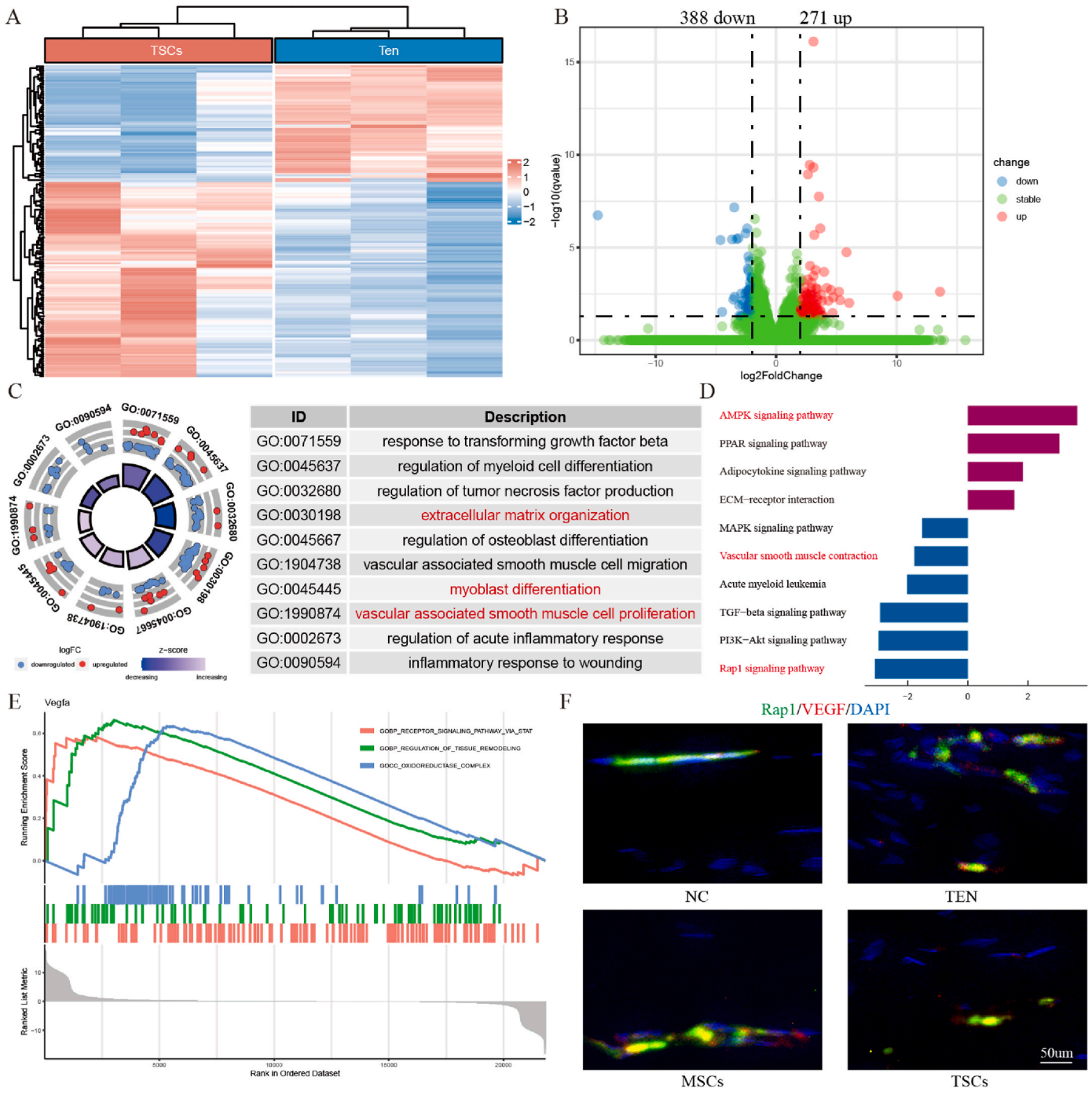

Fig. 7. RNA-seq analysis of tissue mRNA comparing the TSCs and tendinopathy groups at 4 weeks after treatment in a rat model of tendinopathy. (A) Heatmap distribution and (B) volcano plot (388 down-regulated DEGs and 271 up-regulated DEGs) of the TSCs and tendinopathy groups. (C) GO analysis of DEGs indicated that TSCs regulated tendon repair through genes associated with myoblast differentiation, vascularization, and extracellular matrix. (D) KEGG enrichment analysis of target genes showed that TSCs promoted tendon repair through Rap1, AMPK and vascularization signaling pathways. (E) GSEA analysis showed enrichment of the vascularization gene VEGF-A. (F) Relative fluorescence expression of Rap1 and VEGF. Scale bar = 50 μm.

injection therefore induces tissue alterations that are closely coordinated with the pathophysiological modifications seen in human tendinopathy, extending beyond simple tendinitis characterized by inflammatory infiltration. For these reasons, it is also one of the most commonly used approach for modeling tendinopathy in animals [64]. Perhaps one of the most important functions of TSCs driving tendon repair in this study is their ability to inhibit neovascularization, which is now recognized as an early-stage indicator of pathological transformation in tendinopathy. Pathological angiogenesis disrupts normal tendon structure, particularly in the pattern and amount of type III collagen deposition, causing the tendon tissue to lose its original structural and mechanical properties [5,7]. Observations from clinical studies suggest that patients with Achilles tendinopathy have considerably increased levels of neovascularization [65]. Findings from preclinical models also suggest greatly elevated levels of VEGF, a primary growth factor associated with angiogenesis, in rats with tendinopathy together with compromised tissue biomechanics [66]. However, an approach to suppress vascularization as a key to tendon tissue

reconstruction in tendinopathy has not been established. Conventional tissue engineering scaffolds, often with porous structures or mechanical characteristics that guide angiogenesis and enhance vascularization, would be beneficial in the majority of tissue regeneration applications but are not suitable for tendon repair [67,68]. This is because they are unable to prevent excessive activation of neovascularization during the early stages of tendon healing, and moreover often further stimulate stem cell vascular differentiation and vascular endothelial cell angiogenesis [69,70]. In our study, the modified mechanical stimulation provided by microcarriers enhanced the paracrine function of TSCs. This contributed to suppressing VEGF receptor expression in vascular endothelial cells and limiting cell proliferation, migration, and tube-forming capacity. Transcriptome sequencing of collected tissues from the tendinopathy animal model revealed that TSC treatment reduced the proliferation and migration of vascular smooth muscle cells, suggesting that the effects of TSCs in limiting excessive neovascularization could be replicated *in vivo*, which facilitated the improved repair of injured tendon tissues during the early stages of tendon healing.

With their unique ability to inhibit pathological vascularization in tendon repair, the molecular mechanisms activated by TSCs were revealed by secretome analysis. The ability of TSCs to reduce endothelial cell growth and angiogenic factor expression is presumably conveyed through the heightened paracrine activity of MSCs within the TSCs. One of the mechanisms revealed by transcriptome sequencing was downregulation of Rap1 in the TSCs group. This molecule serves a distinctive role in vascular development [71], and its downregulation in the presence of TSCs might help to inhibit overactivation of neovascularization in the early stages of tendon healing. Possibly complementing this was the effect of TSCs in downregulating VEGF, a major regulator of the angiogenic response in endothelial cells. Although the exact role of VEGF in the progression of tendinopathy is unclear, Rap1 signaling is known to mediate proper vascular permeability to VEGF during angiogenesis [72,73]. In our study, elevated Rap1 expression was seen in regions with high levels of VEGF expression, and TSCs were also seen to suppress VEGF, suggesting that the anti-angiogenic effects of TSCs might at least be partly mediated through Rap1. Interestingly, these anti-angiogenic effects appear to contradict our earlier experimental findings, where MSCs loaded in 3D injectable microspheres were shown to stimulate tissue angiogenesis and promote recovery in lower limb ischemia [42]. The critical factor driving this difference might be that the former study focused on direct endothelial differentiation of MSCs within the microspheres, while in this study the improved tendon repair was mainly the result of enhanced paracrine function of MSCs within the TSCs. It is not clear how the increased paracrine function of TSCs could reduce the receptor expression of vascular endothelial cells and further inhibit their angiogenesis potential. The detailed underlying mechanisms warrant further investigation, but are likely associated with the robust ability of MSCs to change their function and secretory behavior in response to biochemical and biophysical conditioning.

Based on our previous findings and studies by others, we hypothesize that one mechanism by which TSCs may prevent VEGF receptor (VEGFR) activation is through enhanced production of TSP1. Moreover, the mechanism by which TSCs regulate angiogenesis in tendon healing may involve the modulation of Rap1, TSP1, and VEGF or VEGFR expression. TSP1 is linked to decreased VEGFR expression [74], whereby it inhibits phosphorylation of VEGFR through CD36 activation, and VEGFR activation is the key to endothelial cell angiogenesis [75]. In addition, CD36 activation interferes with VEGF-dependent nitric oxide-driven angiogenesis [76]. In line with these interactions, our earlier work suggested a significant increase in TSP1 secretion from MSCs that were cultured in microcarriers [44]. In view of these findings, it is possible that an enhanced production of TSP1 from the TSCs in this study was at least partly responsible for preventing VEGFR activation and inhibiting angiogenesis. Separately, Rap1 inactivation inhibits VEGF-VEGFR activation and endothelial cell chemotaxis, hence reducing vascularization [73]. Our immunofluorescence data also demonstrated co-localization of Rap1 and VEGF during *in vivo* tendon healing. We will investigate the precise mechanisms by which TSCs may modulate angiogenesis in tendon repair in our next-step large animal studies, including the potential interactions between Rap1 and TSP1 in this system.

There are some limitations of our study that should be considered for progressing the TSCs toward practical applications in tendon repair. Firstly, we acknowledge that the responses of MSCs in 3D TSCs may not have been directly comparable to 2D MSCs grown on tissue culture plastic due to differences in the material substrate. However, even if the 2D group was grown on a flat gelatin layer, these MSCs would still be transplanted as 'free MSCs' which are fundamentally different to the tissue engineered MSC-microcarrier constructs. It would have been meaningful from a mechanistic perspective to investigate the responses of MSCs on a 2D gelatin-coated surface compared to MSCs within the TSCs, but the 2D gelatin coating would be in the form of a gel that has greatly different material properties compared to the solid structure of the microcarriers. It was not possible in this study to fabricate a 2D layer of gelatin that had the same microscopic structure, stiffness, surface chemistry, and other material parameters as the 3D microcarriers to single out the effects of 2D versus 3D culture. Therefore, we chose to compare the 3D TSCs as tissue engineered MSC constructs in treating tendinopathy, against MSCs derived from traditional 2D plastic culture (similar to those currently being used in clinical studies). We will attempt to remove the confounding influences of differences in material substrate between 3D TSCs and 2D MSCs in our follow-up mechanistic studies. Moreover, we only controlled the initial cell number used for 2D and 3D culture in this study prior to *in vivo* injection, rather than align the total injected cell number between the two groups. This was because cells in the TSCs group would have proliferated since seeding on the microcarriers and produced ECM to form a tissue-engineered construct before being injected *in vivo*. The effects of TSCs on tissue repair are therefore not fundamentally dependent on the number of cells present but rather on the change in paracrine activity of the cells. The progression of cell proliferation was also not comparable between the 2D and 3D groups, since the cells within 3D TSCs would demonstrate higher proliferation potential shortly after seeding due to the more conducive 3D environment, followed by slowing of proliferation as they produce more ECM and form a microtissue construct. Proliferation in the 2D cultured free MSCs is not affected by this process of microtissue formation. For these reasons, only the initial seeded cell number was normalized between the 2D MSCs and 3D TSCs groups for *in vivo* injection.

Secondly, our results suggested that TSCs may improve healing in tendinopathy through multiple enhanced paracrine effects, such as by upregulating tenogenesis and downregulating vascularization. However, there may be a myriad of secretory products from the TSCs mediating these effects, many of which may act in concert, and despite detailed pathway analyses we have not identified the key effector molecules leading to specific protein or molecular level modification. The identification of specific regulatory pathways enabled by TSCs in tendon repair may be warranted in future investigations. Alternative possibilities underlying enhanced repair outcomes by TSCs relating to the effects of 3D culture on MSCs should also be investigated in future studies, for instance, prolonged MSC survival or reduced senescence in addition to changes in their paracrine activity. Thirdly, unlike for osteogenesis, adipogenesis, or chondrogenesis which are natural lineages of differentiation for the hUC-MSCs within TSCs, their capacity for tenogenic differentiation is limited and likely in this study were constrained in their ability to induce rapid tendon repair. Although we already saw that TSCs conveyed tenogenic effects through their paracrine activities, these effects may be greatly enhanced with the future addition of dedicated tenogenic factors such as fibroblast growth factor (FGF) or other auxiliary treatments. For instance, based on our study findings, MSCs or TSCs combined with anti-VEGF antibodies may be a new direction of investigation for treating tendinopathy by controlling pathological

neovascularization. Finding the optimal therapeutic concentration for these additional factors may be critical to successful treatment.

In this study, we selected collagenase injection for modeling tendinopathy, which replicates many of the pathological features of tendon disease, and is a simple and reproducible model suitable for investigating treatment efficacy [64]. Nevertheless, to enable translation, the effects of TSCs treatment will need to be verified in different types of tendinopathy models as well as in large animals. Further verification of protein-level expression of markers related to tendon remodeling and vascularization in large animals, as well as correlation with gene expression data would be beneficial for identifying specific molecular pathways associated with tendon repair through TSCs treatment, in a context relevant to human tendon pathophysiology. Natural tendon repair is divided into three stages: inflammation (1–2 weeks after injury), proliferation (2–6 weeks after injury), and remodeling (4–6 weeks after injury), followed by long-term repair (beyond 6 weeks, lasting 1–2 years) [51]. In this study, we selected 6 weeks after disease injury as the outcome endpoint, which is in the proliferative phase of tendinopathy. Our findings suggest that TSCs may help with tissue healing in the early stage of tendon repair, while their effects during the later stages warrant further investigation. Nevertheless, this study underscores the potential benefit and practicality of employing tissue engineered MSC-microcarrier constructs as a new approach for the treatment of tendinopathy.

4. Conclusion

In this study, TSCs were shown to effectively promote tissue repair in tendinopathy, owing to the paracrine activities of MSCs grown within gelatin microcarriers to inhibit local inflammation and neovascularization while promoting tendon tissue anabolism. Transcriptome sequencing analysis revealed that Rap1 might be a vital pathway involved in the reparative effects of TSCs during tendon healing. The TSCs in this study provide an innovative approach for treating early-stage tendinopathy, importantly by suppressing vascularization as an indicator of pathological progression, and suggest new directions for the design of tissue engineered constructs intended for tendon repair and regeneration.

5. Materials and methods

5.1. Rats and experimental design

All studies were approved by the Ethics Committee of the Animal Care and Use Committee of Shanxi Medical University (Approval Number: DW2023008). A total of 42 male Sprague Dawley rats were purchased from the Laboratory Animal Center of Shanxi Medical University (Taiyuan, China). Six rats were 3 weeks old and were used to extract tenocytes. The remaining 36 rats (200–250 g) were used to establish a tendinopathy model through collagenase I injection in the Achilles tendon. After 1 week of adapting to the environment with ad libitum access to food and water, the 36 rats were randomly divided into 4 groups: control (unoperated), TEN (untreated tendinopathy), MSCs (tendinopathy treated with MSCs grown in 2D), TSCs (tendinopathy treated with MSCs grown in microcarriers).

5.2. Isolation and culture of tenocytes

All procedures and protocols for the acquisition, isolation, and culture of tenocytes were conducted with the approval of the Ethics Committee of the Second Affiliated Hospital, School of Medicine, Shanxi University. Achilles tendon from 3-week old rats were cut into small pieces ($<1\ mm^3$) and digested in 2 mg/mL collagenase type I (Sigma) for 1 h at 37 °C. The digestion was terminated with an equal volume of expansion medium, comprising DMEM supplemented with 10 % fetal bovine serum (FBS, Gibco) and 1 % penicillin/streptomycin. Cells were collected after centrifugation at 178*g* for 5 min and suspended in the expansion medium. Cells were cultured in expansion medium for 5–7 days at 37 °C and 5 % CO_2, and passaged every 2–3 days when the confluence reached approximately 80–90 % with 0.25 % trypsin EDTA (Gibco). Tenocytes at passages 2 to 4 were used for the subsequent experiments.

5.3. Preparation of TSCs

Gelatin microcarriers (GM) (CytoNiche Biotech, China) were provided as dispersible tablets (20mg/tablet). hUC-MSCs (CytoNiche Biotech, China) were cultured in MSC growth medium (CytoNiche Biotech, China). Once the cells reached 80–90 % confluence, they were digested, centrifuged, and suspended in growth medium. To seed MSCs onto GMs, 200 μL of cell suspension (5×10^5 cells) was slowly dropped onto GMs until thorough auto-absorption, and incubated at 37 °C for 2 h to allow cell attachment. Growth medium was then added to culture MSCs in GMs for 1, 3 and 5 days in a cell culture dish. The culture medium was replaced with 50 % fresh medium every 2 days.

5.3.1. Scanning electron microscopy (SEM)

SEM was used to study the microstructure of GMs. Samples were fixed for 12 h at 4 °C with 2.5 % glutaraldehyde in phosphate buffered saline (PBS, pH 7.4), and then rinsed in PBS three times. All samples were dehydrated in a gradient of ethanol (50–100 %), dried to the critical point, and sputtered coated with gold for 2 min at 20 mA. SEM imaging (Hitachi S–3000 N) was performed.

5.4. Cell viability assay

Calcein acetoxymethyl ester (Calcein-AM) and propidium iodide (PI) were used for live/dead staining. Cell viability for MSCs grown in conventional 2D culture (MSCs group) or in 3D TSCs (TSCs group) was visualized by live/dead staining at 1, 3 and 5 days. At each time point, samples were washed three times with PBS, incubated in 100 μL Calcein-AM staining working solution for 30 min at room temperature, washed another three times with PBS, and incubated in 100 μL PI staining working solution for 30 min in the dark. The distribution and viability of cells were observed with a laser scanning confocal microscope (CM1950, Leica, Germany). The viable cells showed green fluorescence, and dead cells showed red fluorescence.

5.5. Cell proliferation, reactive oxygen species (ROS) and senescence assays

Cell proliferation was assessed using EDU assay. Cells were treated with 50 mM 5-ethynyl-2′- deoxyuridine (EdU) (Ribobio, C00052) followed by incubation for 2 h and fixation with 4 % formaldehyde for 10 min. Glycine decolorization was achieved by incubating for 5 min on a shaker, and permeabilization by adding 0.5 % Triton® X-100 for 10 min. All steps of the assay were performed in the dark. The Apollo staining working solution was set up in accordance with the kit's standards. The proper quantity of staining solution was added to the samples, and the mixture was incubated at room temperature for 30 min. The working solution was then discarded and PBS was used to wash the samples. The reaction solution Hoechst33342 was added and samples were incubated in the dark for 30 min before rinsing with PBS. The stained samples were examined with a fluorescence microscope. Image analysis was performed using ImageJ software. Three representative images were selected from different areas of each sample for quantitative analysis.

To assess intracellular ROS levels, cells were incubated with 10 μM DCFH-DA (Beyotime). Fluorescence images were captured using a microscope. Fluorescence quantification was performed using ImageJ.

To assess cell senescence, the SA-β-Gal-positive cell ratios were determined using a senescence detection kit, according to the manufacturer's protocol (Solarbio, G1580). Briefly, samples were washed

with PBS and fixed with kit fixative for 15 min at room temperature, after which the fixative was aspirated and samples were washed three times with PBS. The working solution was set up according to the manufacturer's instructions, added to the samples, and the culture plate was covered with parafilm followed by overnight incubation at 37 °C. On the next day, 2 mL PBS was added to the staining working solution, and samples were examined under a microscope.

5.6. Angiogenesis assays

In vitro angiogenesis assays were conducted using the human endothelial cell line Ea. hy926, which were treated with conditioned medium (CM) derived from the culture medium used to grow MSCs or TSCs: 1) CM^{2D} group (CM from 2D MSC culture); 2) CM^{TSCs} group (CM from TSCs).

For the tube formation assay, 48-well plates were seeded with Ea. hy926 cells at a density of 2.5×10^4 cells/well and cultured for 4 h in basal medium added with the two types of CM. The samples were imaged by microscopy, and the total branch points and tube length were quantified using Image J.

For the transwell migration assay, Ea. hy926 cells at a density of 2.5×10^4 cells/well were seeded into the top chamber of a 24-well, 8 μm pore-size transwell plate, and incubated with the two types of CM in the lower chamber for 4 h. Migrated cells that moved through the membrane pores were fixed with 4 % (w/v) PFA for 20 min and stained with 0.1 % (w/v) crystal violet for 10 min. Unmigrated cells that remained in the top chamber were removed using cotton swabs. An inverted microscope was used for imaging, and the ImageJ program was used to count the number of migrated cells from the microscopy images.

For the scratch wound assay, Ea. hy926 cells at a density of 5×10^5 cells/well were seeded into 6-well plates and grown until confluent. A sterile pipette tip was used to make a scratch in the confluent layer of cells. After washing, the cells were cultured in basal medium added with the two types of CM. At 0, 6 and 12 h, the wound area was imaged and the migration area (%) was computed using Image J.

5.7. Western blot

Protein expression levels of vascular endothelial growth factor receptor 1 (VEGFR1) (ab32152, Abcam, USA), proliferating cell nuclear antigen (PCNA) (13110T, Cell signaling technology, USA), and GAPDH (ab8245, Abcam, USA) in human endothelial cells were measured by western blot. Total proteins were directly extracted with radio immune precipitation assay (RIPA) lysis buffer (P0013B, Beyotime, China) combined with a cocktail of protease inhibitors (AR1192, Boster, China). Protein concentration was calculated using the BCA Protein Assay Kit (AR1189, Boster, China). Proteins were separated on 10 % SDS/PAGE gels (PG112, Epizyme, China) and transferred onto a PVDF membrane (IPVH00010, Millipore, Ireland). The membranes were blocked with 5 % non-fat dry milk and further incubated with the appropriate antibodies. ECL reagent (P0018AS, Beyotime, China) was used to generate chemiluminescent signals using the ChemiDoc XRS + System with Image Lab software (Bio-Rad, USA).

5.8. Bulk RNA-seq and qRT-PCR

For bulk RNA-seq, three replicates per group were collected for mRNA sequencing analysis. In our earlier study, human MSCs delivered through intra-articular injection disappeared at 3 weeks after injection [36]. In this study, animal sampling for RNA-seq was conducted at 4 weeks following treatment, where sample tissues were confirmed to be of rat origin (Table S1, Supporting Information). Total RNA was extracted from tissue samples using the TRIzol reagent (15,596,018, Invitrogen, USA) following the manufacturer's instructions. The RNA was reverse transcribed to create cDNA libraries (Sangon Biotech, China) for sequencing after checking for RNA purity. Samples with biological replicates were analyzed with DESeq2. The filter conditions used to obtain significant differences of differentially expressed genes (DEGs) were: The value of q was defined as the difference between two comparison samples or comparison groups in at least one sample, expressed as 5 or more, and the differences between multiple | Fold-change | 2 or more. Gene Ontology (GO) and Kyoto Encyclopedia of Genes and Genomes (KEGG) enrichment analyses were performed on the DEGs using the "cluster Profiler" R software package, with $p < 0.05$ as the significance criteria.

For qRT-PCR, total RNA was extracted from cell or tissue samples using TRIzol, and cDNA synthesis was performed using a kit in accordance with the manufacturer's instructions (Sangon Biotech, China). SYBR GreenMix (Takara, RR480 (R420A)) was used to measure gene expression by qRT-PCR (Quant Studio 6 Flex, Applied Biosystems, Inc. USA). Relative gene expression levels were computed using the comparative Ct ($2^{-\Delta\Delta CT}$) approach, and all genes were normalized to the internal reference gene GAPDH. Primer sequences are presented in Table S2, Supporting Information.

5.9. Immunofluorescence staining

For immunofluorescence staining of cells grown within TSCs, the microcarriers were dissolved with 3D FloTrix Digest (CNR001-500, CytoNiche Biotech, China) reagent at a ratio of 0.15 mL per mg microcarriers for 15 min at 37 °C. Following lysis, the cells were seeded in a culture plate and fluorescence staining was performed immediately after the cells have attached.

Cell or tissue samples for immunofluorescence staining were fixed in 4 % (w/v) PFA for 30 min, permeabilized with 1 % (v/v) TritonX-100 PBS for 10 min, and then closed with 1 % BSA (w/v) for 30 min. The samples were incubated with primary antibodies overnight at 4 °C. The primary antibodies used were: anti-COL1 (Abcam, ab270993, UK), anti-COL3 (Bioss, bs-0549 R, China), anti-MMP3 (Abcam, ab52915, UK), and anti-MMP13 (Abcam, ab39012, UK). After washing three times with PBS, the samples were incubated with secondary antibodies in the dark at room temperature for 1 h, and finally covered with DAPI (C1005, Beyotime, China) for 30 min. Immunofluorescence images were obtained by confocal microscopy (CM1950, Leica, Germany). Image analysis was performed using ImageJ software. Three representative images were selected from different areas of each sample for quantitative analysis, where the regions of interest (ROIs) should be representative of cell morphology in cell samples or tissue structure for tissue samples.

5.10. Co-culture model of tendinopathy using rat tenocytes and MSCs

The co-culture model was established using a transwell system in 6-well culture plates, with rat tenocytes (TC) seeded into the top chamber and 2D MSCs (adherent) or 3D TSCs (suspension) grown in the bottom chamber. The TCs and MSCs/TSCs were physically separated and only interacting through secreted products in the shared culture medium. The culture medium was DMEM supplemented with 10 % FBS and 1 % penicillin/streptomycin, and IL-1β (10 ng/mL) was added to the wells to provide inflammatory stimulation representative of tendinopathy. The co-cultures were maintained for 2 days at 37 °C and 5 % CO_2, after which cells were subjected to qRT-PCR and immunofluorescence analyses.

5.11. In vivo model of tendinopathy

A total of 36 male Sprague-Dawley adult rats (body weight 200–250 g) were used for *in vivo* experiments. Except for the control group, all rats were deeply anesthetized with 1 % pentobarbital sodium (0.05 g/kg), and subsequently injected with 60 μL collagenase I solution (5 mg/mL) in the right hind leg every 3 days. After 14 days, the tendinopathy model was successfully established and rats were divided into the TEN, MSCs,

and TSCs groups for the following treatments.

All hUC-MSCs were cultured in serum-free medium and resuspended at a density of 1×10^7 cells/mL. For the TSCs group, 200 μL cell suspension was seeded to GM and cultured for 3 days (per results shown in Section 2.1) before the TSC constructs were injected into animals. For the MSCs group, 200 μL cell suspension was cultured in 2D for 3 days and then injected into animals as a cell suspension. The tendinopathy group received the same volume of serum-free medium by injection as the TSCs and MSCs groups without cells, while the blank control group received no care. Four weeks after treatment, the recovery of Achilles tendon was evaluated by behavioral and histological analysis. All experiments were performed using nine independent samples per group.

5.12. Reflexive-based sensory testing

At 4 weeks after rats were treated with MSCs or TSCs, they were subjected to sensory and motor function testing prior to sacrifice. The weight bearing test was carried out using a capacitance meter (Model 600, IITC Life Sciences, Woodland Hills, California, USA) to assess the willingness to apply weight to the Achilles tendon. The weight distribution was measured in grams by placing each of the rear paws on a sensor pad. The percentage of weight applied to the injured leg was calculated. To measure mechanical sensitivity, rats were segregated into a separate chamber with an opaque barrier on a raised grid, preventing them from seeing or interacting with one another. A succession of von Frey fibers with logarithmically increasing stiffness was used to stimulate the rat hind paw, by placing the fiber perpendicular to the central surface of the plantar foot. The upper and lower threshold of 50 % paw extraction was calculated.

A small animal gait analyzer (CatWalk) was used to test the return of motor function. The rats were allowed to adapt to their surroundings in the dark before being placed on the small animal gait analyzer runway, which had pre-determined rat gait parameters (camera gain (dB): 25.30, green intensity threshold: 0.10, red ceiling light (V): 17.6, green walkway light (V): 18.9, maximum range from: 50 to 180, frames before delta: 5, intensity minimum: 85). Gait characteristics during the process of passing the runway were recognized based on the pressure generated by the rat limbs as they crossed the fixed runway in the fixed detection region at a consistent speed. Each set of measurement data was repeated three times and the average value was used as the measurement result.

5.13. Macroscopic examination and analysis of tendon adhesion

Collected tendons were macroscopically examined, and assessed for the severity and extent of tendon adhesion. The level of tendon adhesion was graded from 1 to 5 according to a previously reported adhesion grading system [54]: 1, almost no adhesions; 2, filamentous adhesion easily separated by blunt dissection; 3, less than or equal to 50 % of the adhesion area required for sharp dissection; 4, 51–97.5 % of the adhesion area required for sharp dissection; 5, more than 97.5 % of the adhesion area required for sharp dissection.

5.14. Histopathological analysis

Collected tendon specimens were fixed in 4 % (w/v) paraformaldehyde (PFA) for 24 h and dehydrated using an alcohol gradient, followed by embedding in paraffin. Histological sections (5 μm) were prepared using a microtome (Leica). Sections were stained by Masson staining and hematoxylin-eosin (HE). For immunofluorescence, sections were cleaned three times with TBST, added with 0.5 % Triton X-100, and then blocked with 5 % bovine serum albumin (BSA) for 30 min at room temperature. Stained images were captured using a confocal microscope (Panorama MIDI, 3DHistech, Hungary). Image analysis was performed using ImageJ software. Three representative images were selected from different areas of each sample for quantitative analysis, where the regions of interest (ROIs) should be representative of tissue structure for tissue samples.

Histological scoring was performed using a previously reported grading system [30]. The scale includes six characteristics, each of which is graded 0, 1, 2, or 3: (1) Fiber arrangement; (2) Fiber structure; (3) Nuclear round degree; (4) Inflammation cells; (5) Number of blood vessels; and (6) Cell density. A score of 0 points represented normal, while 3 points represented maximally abnormal. Three histologists randomly chose three sections from each sample for evaluation.

5.15. Statistical analysis

Statistical analysis was performed using SPSS 11.0, and visualized using GraphPad Prism 9. All quantitative data were presented as mean ± standard deviation (SD). All experiments were performed using at least three independent samples. The unpaired two-tailed student's t-test (for two groups) and one-way ANOVA with Tukey's multiple comparisons (for more than two groups) were performed to analyze data with normal distribution and equal variances. Mann-Whitney *U* test (for two groups) and Kruskal-Wallis H-test with Dunn's multiple comparisons (for more than two groups) were performed to analyze non-parametric data. $p < 0.05$ was considered statistically significant (*$p < 0.05$, **$p < 0.01$, ***$p < 0.001$, and ****$p < 0.0001$).

Ethics approval and consent to participate

All studies了 were approved by the Ethics Committee of the Animal Care and Use Committee of Shanxi Medical University (Approval Number: DW2023008)

All procedures and protocols for the acquisition, isolation, and culture of tenocytes were conducted with the approval of the Ethics Committee of the Second Affiliated Hospital, School of Medicine, Shanxi University.

Funding

This study was supported by the National Natural Science Foundation of China (81802204) and by Zhejiang University School of Medicine, The First Affiliated Hospital's Foundation (G2022010-18), Alibaba Cloud, Zhejiang Medical and Health Science and Technology Project (2023RC010), Natural Science Foundation of Zhejiang Province (LTGY23H060007) and National Health and Medical Research Council (NHMRC, Australia; GNT1120249).

CRediT authorship contribution statement

Dijun Li: Writing – review & editing, Writing – original draft, Methodology, Formal analysis, Data curation, Conceptualization. **Jingwei Jiu:** Software, Data curation, Conceptualization. **Haifeng Liu:** Writing – review & editing, Methodology, Conceptualization. **Xiaojun Yan:** Writing – review & editing, Resources. **Xiaoke Li:** Visualization, Software, Data curation. **Lei Yan:** Methodology, Conceptualization. **Jing Zhang:** Writing – review & editing, Investigation. **Zijuan Fan:** Methodology. **Songyan Li:** Investigation, Conceptualization. **Guangyuan Du:** Investigation, Conceptualization. **Jiao Jiao Li:** Writing – review & editing, Funding acquisition, Conceptualization. **Yanan Du:** Writing – review & editing. **Wei Liu:** Resources. **Bin Wang:** Supervision, Funding acquisition, Conceptualization.

Declaration of competing interest

The authors declare the following financial interests/personal relationships which may be considered as potential competing interests:

Xiaojun Yan and Wei Liu are employees of Beijing CytoNiche Biotechnology Co. Ltd. The other authors declare that we have no financial and personal relationships with other people or organizations that can inappropriately influence our work.

Acknowledgements

We gratefully acknowledge Yuanyuan Zhang for their assistance in preparing the microcarriers and providing technical support. We also thank Dr Hongsheng Yu from the Tsinghua University for technical assistance.

Appendix A. Supplementary data

Supplementary data to this article can be found online at https://doi.org/10.1016/j.bioactmat.2024.06.029.

References

[1] G. Nourissat, F. Berenbaum, D. Duprez, Tendon injury: from biology to tendon repair, Nat. Rev. Rheumatol. 11 (4) (2015) 223–233, https://doi.org/10.1038/nrrheum.2015.26.
[2] S.P. Magnusson, H. Langberg, M. Kjaer, The pathogenesis of tendinopathy: balancing the response to loading, Nat. Rev. Rheumatol. 6 (5) (2010) 262–268, https://doi.org/10.1038/nrrheum.2010.43.
[3] R.J. de Vos, A.C. van der Vlist, J. Zwerver, D.E. Meuffels, F. Smithuis, R. van Ingen, F. van der Giesen, E. Visser, A. Balemans, M. Pols, N. Veen, M. den Ouden, A. Weir, Dutch multidisciplinary guideline on Achilles tendinopathy, Br. J. Sports Med. 55 (20) (2021) 1125–1134, https://doi.org/10.1136/bjsports-2020-103867.
[4] C. Loiacono, S. Palermi, B. Massa, I. Belviso, V. Romano, A. Di Gregorio, F. Sirico, A.M. Sacco, Tendinopathy: pathophysiology, therapeutic options, and role of nutraceutics. A narrative literature review, Medicina 55 (8) (2019), https://doi.org/10.3390/medicina55080447.
[5] N.L. Millar, K.G. Silbernagel, K. Thorborg, P.D. Kirwan, L.M. Galatz, G.D. Abrams, G.A.C. Murrell, I.B. McInnes, S.A. Rodeo, Tendinopathy, Nat. Rev. Dis. Prim. 7 (1) (2021) 1, https://doi.org/10.1038/s41572-020-00234-1.
[6] P.P. Lui, N. Maffulli, C. Rolf, R.K. Smith, What are the validated animal models for tendinopathy? Scand. J. Med. Sci. Sports 21 (1) (2011) 3–17, https://doi.org/10.1111/j.1600-0838.2010.01164.x.
[7] D. Docheva, S.A. Müller, M. Majewski, C.H. Evans, Biologics for tendon repair, Adv. Drug Deliv. Rev. 84 (2015) 222–239, https://doi.org/10.1016/j.addr.2014.11.015.
[8] M.A. Childress, A. Beutler, Management of chronic tendon injuries, Am. Fam. Physician 87 (7) (2006) 486–490.
[9] B.M. Andres, G.A. Murrell, Treatment of tendinopathy: what works, what does not, and what is on the horizon, Clin. Orthop. Relat. Res. 466 (7) (2008) 1539–1554, https://doi.org/10.1007/s11999-008-0260-1.
[10] J.H. Shepherd, H.R.C. Screen, Fatigue loading of tendon, Int. J. Exp. Pathol. 94 (4) (2013) 260–270, https://doi.org/10.1111/iep.12037.
[11] C.N. Maganaris, M.V. Narici, L.C. Almekinders, N. Maffulli, Biomechanics and pathophysiology of overuse tendon injuries ideas on insertional tendinopathy, Sports Med. 34 (14) (2004) 1005–1017.
[12] P.W. Ackermann, P.T. Salo, D.A. Hart, Neuronal pathways in tendon healing, Front. Biosci. 14 (2009) 5165–5187.
[13] T.A.H. Järvinen, Neovascularisation in tendinopathy: from eradication to stabilisation? Br. J. Sports Med. 54 (1) (2020) 1–2, https://doi.org/10.1136/bjsports-2019-100608.
[14] S. Kokubu, R. Inaki, K. Hoshi, A. Hikita, Adipose-derived stem cells improve tendon repair and prevent ectopic ossification in tendinopathy by inhibiting inflammation and inducing neovascularization in the early stage of tendon healing, Regenerative therapy 14 (2020) 103–110, https://doi.org/10.1016/j.reth.2019.12.003.
[15] T. Pufe, W.J. Petersen, R. Mentlein, B.N. Tillmann, The role of vasculature and angiogenesis for the pathogenesis of degenerative tendons disease, Scand. J. Med. Sci. Sports 15 (4) (2005) 211–222, https://doi.org/10.1111/j.1600-0838.2005.00465.x.
[16] R.H. Gelberman, S.W. Linderman, R. Jayaram, A.D. Dikina, S. Sakiyama-Elbert, E. Alsberg, S. Thomopoulos, H. Shen, Combined administration of ASCs and BMP-12 promotes an M2 macrophage phenotype and enhances tendon healing, Clin. Orthop. Relat. Res. 475 (9) (2017) 2318–2331, https://doi.org/10.1007/s11999-017-5369-7.
[17] R. Aicale, R.D. Bisaccia, A. Oliviero, F. Oliva, N. Maffulli, Current pharmacological approaches to the treatment of tendinopathy, Expet Opin. Pharmacother. 21 (12) (2020) 1467–1477, https://doi.org/10.1080/14656566.2020.1763306.
[18] N.A.C. van den Boom, M. Winters, H.J. Haisma, M.H. Moen, Efficacy of stem cell therapy for tendon disorders: a systematic review, Orthopaedic journal of sports medicine 8 (4) (2020) 2325967120915857, https://doi.org/10.1177/2325967120915857.
[19] A.I. Caplan, D. Correa, The MSC: an injury drugstore, Cell Stem Cell 9 (1) (2011) 11–15, https://doi.org/10.1016/j.stem.2011.06.008.
[20] A.C. Bowles, D. Kouroupis, M.A. Willman, C. Perucca Orfei, A. Agarwal, D. Correa, Signature quality attributes of CD146(+) mesenchymal stem/stromal cells correlate with high therapeutic and secretory potency, Stem Cell. 38 (8) (2020) 1034–1049, https://doi.org/10.1002/stem.3196.
[21] D. Jovic, Y. Yu, D. Wang, K. Wang, H. Li, F. Xu, C. Liu, J. Liu, Y. Luo, A brief overview of global trends in MSC-based cell therapy, Stem cell reviews and reports 18 (5) (2022) 1525–1545, https://doi.org/10.1007/s12015-022-10369-1.
[22] Z. Zhao, Z. Wang, G. Li, Z. Cai, J. Wu, L. Wang, L. Deng, M. Cai, W. Cui, Injectable microfluidic hydrogel microspheres for cell and drug delivery, Adv. Funct. Mater. 31 (31) (2021), https://doi.org/10.1002/adfm.202103339.
[23] F. Migliorini, M. Tingart, N. Maffulli, Progress with stem cell therapies for tendon tissue regeneration, Expet Opin. Biol. Ther. 20 (11) (2020) 1373–1379, https://doi.org/10.1080/14712598.2020.1786532.
[24] Z. Chen, P. Chen, M. Zheng, J. Gao, D. Liu, A. Wang, Q. Zheng, T. Leys, A. Tai, M. Zheng, Challenges and perspectives of tendon-derived cell therapy for tendinopathy: from bench to bedside, Stem Cell Res. Ther. 13 (1) (2022), https://doi.org/10.1186/s13287-022-03113-6.
[25] T. Lei, T. Zhang, W. Ju, X. Chen, B.C. Heng, W. Shen, Z. Yin, Biomimetic strategies for tendon/ligament-to-bone interface regeneration, Bioact. Mater. 6 (8) (2021) 2491–2510, https://doi.org/10.1016/j.bioactmat.2021.01.022.
[26] K.T. Shalumon, H.-T. Liao, W.-H. Li, D.T. G, M.P. A, J.-P. Chen, Braided suture-reinforced fibrous yarn bundles as a scaffold for tendon tissue engineering in extensor digitorum tendon repair, Chem. Eng. J. 454 (2023), https://doi.org/10.1016/j.cej.2022.140366.
[27] R. Liu, B. Zhou, H. Zhang, Y. Chen, C. Fan, T. Zhang, T. Qin, J. Han, S. Zhang, X. Chen, W. Shen, J. Chang, Z. Yin, Inhibition of ROS activity by controlled release of proanthocyanidins from mesoporous silica nanocomposites effectively ameliorates heterotopic ossification in tendon, Chem. Eng. J. 420 (1) (2021) 129415, https://doi.org/10.1016/j.cej.2021.129415.
[28] J. Jing, Y. Qian Qian, S. Jie, Z. You Lang, Macrophages regulated by cyclooxygenases promote tendon healing via Pla1a/Etv1 axis, Chem. Eng. J. 477 (2023), https://doi.org/10.1016/j.cej.2023.147144.
[29] H. Liu, X. Yan, J. Jiu, J.J. Li, Y. Zhang, G. Wang, D. Li, L. Yan, Y. Du, B. Zhao, B. Wang, Self-assembly of gelatin microcarrier-based MSC microtissues for spinal cord injury repair, Chem. Eng. J. 451 (2023) 138806, https://doi.org/10.1016/j.cej.2022.138806.
[30] H. Zhang, Y. Chen, C. Fan, R. Liu, J. Huang, Y. Zhang, C. Tang, B. Zhou, X. Chen, W. Ju, Y. Zhao, J. Han, P. Wu, S. Zhang, W. Shen, Z. Yin, X. Chen, H. Ouyang, Cell-subpopulation alteration and FGF7 activation regulate the function of tendon stem/progenitor cells in 3D microenvironment revealed by single-cell analysis, Biomaterials 280 (2022) 121238, https://doi.org/10.1016/j.biomaterials.2021.121238.
[31] M. Govoni, A.C. Berardi, C. Muscari, R. Campardelli, F. Bonafè, C. Guarnieri, E. Reverchon, E. Giordano, N. Maffulli, G. Della Porta, An engineered multiphase three-dimensional microenvironment to ensure the controlled delivery of cyclic strain and human growth differentiation factor 5 for the tenogenic commitment of human bone marrow mesenchymal stem cells, Tissue Eng. 23 (15–16) (2017) 811–822, https://doi.org/10.1089/ten.tea.2016.0407.
[32] C. Yang, B. Han, C. Cao, D. Yang, X. Qu, X. Wang, An injectable double-network hydrogel for the co-culture of vascular endothelial cells and bone marrow mesenchymal stem cells for simultaneously enhancing vascularization and osteogenesis, J. Mater. Chem. B 6 (47) (2018) 7811–7821, https://doi.org/10.1039/c8tb02244e.
[33] S.T. Robinson, A.M. Douglas, T. Chadid, K. Kuo, A. Rajabalan, H. Li, I.B. Copland, T.H. Barker, J. Galipeau, L.P. Brewster, A novel platelet lysate hydrogel for endothelial cell and mesenchymal stem cell-directed neovascularization, Acta Biomater. 36 (2016) 86–98, https://doi.org/10.1016/j.actbio.2016.03.002.
[34] M.X. Li, L. Li, S.Y. Zhou, J.H. Cao, W.H. Liang, Y. Tian, X.T. Shi, X.B. Yang, D. Y. Wu, A biomimetic orthogonal-bilayer tubular scaffold for the co-culture of endothelial cells and smooth muscle cells, RSC Adv. 11 (50) (2021) 31783–31790, https://doi.org/10.1039/d1ra04472a.
[35] D.G. Belair, M.J. Miller, S. Wang, S.R. Darjatmoko, B.Y.K. Binder, N. Sheibani, W. L. Murphy, Differential regulation of angiogenesis using degradable VEGF-binding microspheres, Biomaterials 93 (2016) 27–37, https://doi.org/10.1016/j.biomaterials.2016.03.021.
[36] B. Wang, W. Liu, J.J. Li, S. Chai, D. Xing, H. Yu, Y. Zhang, W. Yan, Z. Xu, B. Zhao, Y. Du, Q. Jiang, A low dose cell therapy system for treating osteoarthritis: *In vivo* study and *in vitro* mechanistic investigations, Bioact. Mater. 7 (2022) 478–490, https://doi.org/10.1016/j.bioactmat.2021.05.029.
[37] D.M. Hoang, P.T. Pham, T.Q. Bach, A.T.L. Ngo, Q.T. Nguyen, T.T.K. Phan, G. H. Nguyen, P.T.T. Le, V.T. Hoang, N.R. Forsyth, M. Heke, L.T. Nguyen, Stem cell-based therapy for human diseases, Signal Transduct. Targeted Ther. 7 (1) (2022), https://doi.org/10.1038/s41392-022-01134-4.
[38] Y. Shang, H. Guan, F. Zhou, Biological characteristics of umbilical cord mesenchymal stem cells and its therapeutic potential for hematological disorders, Front. Cell Dev. Biol. 9 (2021) 570179, https://doi.org/10.3389/fcell.2021.570179.
[39] J.H. Yea, Y. Kim, C.H. Jo, Comparison of mesenchymal stem cells from bone marrow, umbilical cord blood, and umbilical cord tissue in regeneration of a full-thickness tendon defect *in vitro* and *in vivo*, Biochem Biophys Rep 34 (2023) 101486, https://doi.org/10.1016/j.bbrep.2023.101486.
[40] T. Wang, Z. Lin, R.E. Day, B. Gardiner, E. Landao-Bassonga, J. Rubenson, T.B. Kirk, D.W. Smith, D.G. Lloyd, G. Hardisty, A. Wang, Q. Zheng, M.H. Zheng, Programmable mechanical stimulation influences tendon homeostasis in a bioreactor system, Biotechnol. Bioeng. 110 (5) (2013) 1495–1507, https://doi.org/10.1002/bit.24809.
[41] R.M. Delaine-Smith, G.C. Reilly, Mesenchymal stem cell responses to mechanical stimuli, Muscles, Ligaments Tendons J. 2 (3) (2012) 169–180.
[42] Y. Li, W. Liu, F. Liu, Y. Zeng, S. Zuo, S. Feng, C. Qi, B. Wang, X. Yan, A. Khademhosseini, J. Bai, Y. Du, Primed 3D injectable microniches enabling low-dosage cell therapy for critical limb ischemia, Proc. Natl. Acad. Sci. USA 111 (37) (2014) 13511–13516, https://doi.org/10.1073/pnas.1411295111.

[43] Y. Zhao, Z. You, D. Xing, J.J. Li, Q. Zhang, H. Huang, Z. Li, S. Jiang, Z. Wu, Y. Zhang, W. Li, L. Zhang, Y. Du, J. Lin, Comparison of chondrocytes in knee osteoarthritis and regulation by scaffold pore size and stiffness, tissue engineering, Part. Accel. 27 (3–4) (2021) 223–236, https://doi.org/10.1089/ten.TEA.2020.0085.

[44] D. Xing, W. Liu, J.J. Li, L. Liu, A. Guo, B. Wang, H. Yu, Y. Zhao, Y. Chen, Z. You, C. Lyu, W. Li, A. Liu, Y. Du, J. Lin, Engineering 3D functional tissue constructs using self-assembling cell-laden microniches, Acta Biomater. 114 (2020) 170–182, https://doi.org/10.1016/j.actbio.2020.07.058.

[45] Y. Zhang, R. Sheng, J. Chen, H. Wang, Y. Zhu, Z. Cao, X. Zhao, Z. Wang, C. Liu, Z. Chen, P. Zhang, B. Kuang, H. Zheng, C. Shen, Q. Yao, W. Zhang, Silk fibroin and sericin differentially potentiate the paracrine and regenerative functions of stem cells through multiomics analysis, Adv. Mater. 35 (20) (2023), https://doi.org/10.1002/adma.202210517.

[46] T.H. Qazi, D.J. Mooney, G.N. Duda, S. Geissler, Biomaterials that promote cell-cell interactions enhance the paracrine function of MSCs, Biomaterials 140 (2017) 103–114, https://doi.org/10.1016/j.biomaterials.2017.06.019.

[47] S. Huang, Y. Wu, D. Gao, X. Fu, Paracrine action of mesenchymal stromal cells delivered by microspheres contributes to cutaneous wound healing and prevents scar formation in mice, Cytotherapy 17 (7) (2015) 922–931, https://doi.org/10.1016/j.jcyt.2015.03.690.

[48] C.-H. Chen, D.-L. Li, A.D.-C. Chuang, B.S. Dash, J.-P. Chen, Tension stimulation of tenocytes in aligned hyaluronic acid/platelet-rich plasma-polycaprolactone core-sheath nanofiber membrane scaffold for tendon tissue engineering, Int. J. Mol. Sci. 22 (20) (2021), https://doi.org/10.3390/ijms222011215.

[49] Y. Bi, D. Ehirchiou, T.M. Kilts, C.A. Inkson, M.C. Embree, W. Sonoyama, L. Li, A. I. Leet, B.-M. Seo, L. Zhang, S. Shi, M.F. Young, Identification of tendon stem/progenitor cells and the role of the extracellular matrix in their niche, Nat. Med. 13 (10) (2007) 1219–1227, https://doi.org/10.1038/nm1630.

[50] Y. Wang, G. He, H. Tang, Y. Shi, X. Kang, J. Lyu, M. Zhu, M. Zhou, M. Yang, M. Mu, W. Chen, B. Zhou, J. Zhang, K. Tang, Aspirin inhibits inflammation and scar formation in the injury tendon healing through regulating JNK/STAT-3 signalling pathway, Cell Prolif. 52 (4) (2019) e12650, https://doi.org/10.1111/cpr.12650.

[51] D. Li, G. Wang, J. Li, L. Yan, H. Liu, J. Jiu, X. Li, J.J. Li, B. Wang, Biomaterials for tissue-engineered treatment of tendinopathy in animal models: a systematic review, Tissue Eng. B Rev. 29 (4) (2023) 387–413, https://doi.org/10.1089/ten.teb.2022.0178.

[52] S. Lomax, P.A. Windsor, Topical anesthesia mitigates the pain of castration in beef calves, J. Anim. Sci. 91 (10) (2013) 4945–4952, https://doi.org/10.2527/jas2012-5984.

[53] S.R. Chaplan, F.W. Bach, J.W. Pogrel, J.M. Chung, T.L. Yaksh, Quantitative assessment of tactile allodynia in the rat paw, J. Neurosci. Methods 53 (1) (1994) 55–63.

[54] S. Liu, M. Qin, C. Hu, F. Wu, W. Cui, T. Jin, C. Fan, Tendon healing and anti-adhesion properties of electrospun fibrous membranes containing bFGF loaded nanoparticles, Biomaterials 34 (19) (2013) 4690–4701, https://doi.org/10.1016/j.biomaterials.2013.03.026.

[55] H. Kim, C. Bae, Y.M. Kook, W.G. Koh, K. Lee, M.H. Park, Mesenchymal stem cell 3D encapsulation technologies for biomimetic microenvironment in tissue regeneration, Stem Cell Res. Ther. 10 (1) (2019) 51, https://doi.org/10.1186/s13287-018-1130-8.

[56] Y. Ma, M. Lin, G. Huang, Y. Li, S. Wang, G. Bai, T.J. Lu, F. Xu, 3D spatiotemporal mechanical microenvironment: a hydrogel-based platform for guiding stem cell fate, Adv. Mater. (Weinheim, Ger.) 30 (49) (2018) e1705911, https://doi.org/10.1002/adma.201705911.

[57] M.S. Rehmann, J.I. Luna, E. Maverakis, A.M. Kloxin, Tuning microenvironment modulus and biochemical composition promotes human mesenchymal stem cell tenogenic differentiation, J. Biomed. Mater. Res. 104 (5) (2016) 1162–1174, https://doi.org/10.1002/jbm.a.35650.

[58] P.J. Yang, M.E. Levenston, J.S. Temenoff, Modulation of mesenchymal stem cell shape in enzyme-sensitive hydrogels is decoupled from upregulation of fibroblast markers under cyclic tension, Tissue engineering, Part. Accel. 18 (21–22) (2012) 2365–2375, https://doi.org/10.1089/ten.TEA.2011.0727.

[59] W. Liu, Y. Li, S. Feng, J. Ning, J. Wang, M. Gou, H. Chen, F. Xu, Y. Du, Magnetically controllable 3D microtissues based on magnetic microcryogels, Lab Chip 14 (15) (2014) 2614–2625, https://doi.org/10.1039/c4lc00081a.

[60] O. Chaudhuri, L. Gu, D. Klumpers, M. Darnell, S.A. Bencherif, J.C. Weaver, N. Huebsch, H.P. Lee, E. Lippens, G.N. Duda, D.J. Mooney, Hydrogels with tunable stress relaxation regulate stem cell fate and activity, Nat. Mater. 15 (3) (2016) 326–334, https://doi.org/10.1038/nmat4489.

[61] Y. Li, Z. Zhong, C. Xu, X. Wu, J. Li, W. Tao, J. Wang, Y. Du, S. Zhang, 3D micropattern force triggers YAP nuclear entry by transport across nuclear pores and modulates stem cells paracrine, Natl. Sci. Rev. 10 (8) (2023) nwad165, https://doi.org/10.1093/nsr/nwad165.

[62] N.L. Millar, G.A.C. Murrell, I.B. McInnes, Inflammatory mechanisms in tendinopathy - towards translation, Nat. Rev. Rheumatol. 13 (2) (2017) 110–122, https://doi.org/10.1038/nrrheum.2016.213.

[63] S.J. Warden, Animal models for the study of tendinopathy, Br. J. Sports Med. 41 (4) (2007) 232–240, https://doi.org/10.1136/bjsm.2006.032342.

[64] J. Luo, Z. Wang, C. Tang, Z. Yin, J. Huang, D. Ruan, Y. Fei, C. Wang, X. Mo, J. Li, J. Zhang, C. Fang, J. Li, X. Chen, W. Shen, Animal model for tendinopathy, Journal of orthopaedic translation 42 (2023) 43–56, https://doi.org/10.1016/j.jot.2023.06.005.

[65] A. De Marchi, S. Pozza, E. Cenna, F. Cavallo, G. Gays, L. Simbula, P. De Petro, A. Masse, G. Massazza, Achilles tendinopathy, the neovascularization, detected by contrast-enhanced ultrasound (CEUS), is abundant but not related to symptoms, Knee Surg. Sports Traumatol. Arthrosc. 26 (7) (2018) 2051–2058, https://doi.org/10.1007/s00167-017-4710-8.

[66] H. Sahin, N. Tholema, W. Petersen, M.J. Raschke, R. Stange, Impaired biomechanical properties correlate with neoangiogenesis as well as VEGF and MMP-3 expression during rat patellar tendon healing, J. Orthop. Res. 30 (12) (2012) 1952–1957, https://doi.org/10.1002/jor.22147.

[67] M.S. Liang, M. Koobatian, P. Lei, D.D. Swartz, S.T. Andreadis, Differential and synergistic effects of mechanical stimulation and growth factor presentation on vascular wall function, Biomaterials 34 (30) (2013) 7281–7291, https://doi.org/10.1016/j.biomaterials.2013.05.073.

[68] X. Zhou, Y. Qian, L. Chen, T. Li, X. Sun, X. Ma, J. Wang, C. He, Flowerbed-inspired biomimetic scaffold with rapid internal tissue infiltration and vascularization capacity for bone repair, ACS Nano 17 (5) (2023) 5140–5156, https://doi.org/10.1021/acsnano.3c00598.

[69] M. Lian, B. Sun, Y. Han, B. Yu, W. Xin, R. Xu, B. Ni, W. Jiang, Y. Hao, X. Zhang, Y. Shen, Z. Qiao, K. Dai, A low-temperature-printed hierarchical porous sponge-like scaffold that promotes cell-material interaction and modulates paracrine activity of MSCs for vascularized bone regeneration, Biomaterials 274 (2021), https://doi.org/10.1016/j.biomaterials.2021.120841.

[70] Y. Tang, K. Luo, J. Tan, R. Zhou, Y. Chen, C. Chen, Z. Rong, M. Deng, X. Yu, C. Zhang, Q. Dai, W. Wu, J. Xu, S. Dong, F. Luo, Laminin alpha 4 promotes bone regeneration by facilitating cell adhesion and vascularization, Acta Biomater. 126 (2021) 183–198, https://doi.org/10.1016/j.actbio.2021.03.011.

[71] G. Carmona, S. Gottig, A. Orlandi, J. Scheele, T. Bauerle, M. Jugold, F. Kiessling, R. Henschler, A.M. Zeiher, S. Dimmeler, E. Chavakis, Role of the small GTPase Rap1 for integrin activity regulation in endothelial cells and angiogenesis, Blood 113 (2) (2009) 488–497, https://doi.org/10.1182/blood-2008-02-138438.

[72] S. Lakshmikanthan, M. Sobczak, S.L. Calzi, L. Shaw, M.B. Grant, M. Chrzanowska-Wodnicka, Rap1B promotes VEGF-induced endothelial permeability and is required for dynamic regulation of endothelial barrier, J. Cell Sci. 131 (1) (2018) jcs207605.

[73] S. Lakshmikanthan, M. Sobczak, C. Chun, A. Henschel, J. Dargatz, R. Ramchandran, M. Chrzanowska-Wodnicka, Rap1 promotes VEGFR2 activation and angiogenesis by a mechanism involving integrin alphavbeta(3), Blood 118 (7) (2011) 2015–2026, https://doi.org/10.1182/blood-2011-04-349282.

[74] D.D. Roberts, P. Fei, I. Zaitoun, M. Farnoodian, D.L. Fisk, S. Wang, C.M. Sorenson, N. Sheibani, Expression of thrombospondin-1 modulates the angioinflammatory phenotype of choroidal endothelial cells, PLoS One 9 (12) (2014), https://doi.org/10.1371/journal.pone.0116423.

[75] W. Choi, A.K. Nensel, S. Droho, M.A. Fattah, S. Mokashi-Punekar, D.I. Swygart, S. T. Burton, G.W. Schwartz, J.A. Lavine, N.C. Gianneschi, Thrombospondin-1 proteomimetic polymers exhibit anti-angiogenic activity in a neovascular age-related macular degeneration mouse model, Sci. Adv. 9 (41) (2023) eadi8534, https://doi.org/10.1126/sciadv.adi8534.

[76] J.S. Isenberg, Y. Jia, J. Fukuyama, C.H. Switzer, D.A. Wink, D.D. Roberts, Thrombospondin-1 inhibits nitric oxide signaling via CD36 by inhibiting myristic acid uptake, J. Biol. Chem. 282 (21) (2007) 15404–15415, https://doi.org/10.1074/jbc.M701638200.